Journal bearing impedance descriptions for rotordynamic applications

D. Childs

Associate Professor of Mechanical Engineering,
The University of Louisville,
Louisville, Ky. Mem. ASME

H. Moes
H. van Leeuwen

Technological University Twente,
Department of Mechanical Engineering,
Enschede, The Netherlands

Journal Bearing Impedance Descriptions for Rotordynamic Applications[1]

Bearing impedance vectors are introduced for plain journal bearings which define the bearing reaction force components as a function of the bearing motion. Impedance descriptions are developed directly for the approximate Ocvirk (short) and Sommerfeld (long) bearing solutions. The impedance vector magnitude and the mobility vector magnitude of Booker are shown to be reciprocals. The transformation relationships between mobilities and impedance are derived and used to define impedance vectors for a number of existing mobility vectors including the finite-length mobility vectors developed by Moes. The attractiveness and utility of the impedance-vector formulation for transient simulation work is demonstrated by numerical examples for the Ocvirk "π", and "2π" bearing impedances and the cavitating finite-length-bearing impedance. The examples presented demonstrate both bearing and squeeze-film damper application. A direct analytic method for deriving a complete set of (analytic) stiffness and damping coefficients from impedance descriptions is developed and demonstrated for the cavitating finite-length-bearing impedances. Analytic expressions are provided for all direct and cross-coupled stiffness and damping coefficients, and compared to previously developed numerical results. These coefficients are used for stability analysis of a rotor, supported in finite-length cavitating bearings. Onset-speed-of-instability results are presented as a function of the L/D ratio for a range of bearing numbers. Damping coefficients are also presented for finite-length squeeze-film dampers.

Introduction

The objective of this work is the development of analytic descriptions for plain circumferentially-symmetric fluid journal bearings which are suitable for use in rotordynamic analysis. Specifically, a description is required which defines the bearing reaction vector as a function of the position and velocity vectors of the rotor at the bearing location. A nonlinear description is required for transient rotordynamic analysis, and stiffness and damping coefficients are required for linear synchronous-rotor-response and stability calculations. Booker [1, 2, 3],[2] Blok [4], and other investigators have considered the inverse problem of defining the velocity vector of a journal bearing as a function of its load and position vectors, and derived "mobility" vectors, which define the pure-squeeze-velocity vector in terms of the load and position vectors. Mobility descriptions have proven to be extremely useful for situations in which the dynamics of the rotor are negligible, and the load applied to the bearing is a known function of time, e.g., bearings of internal combustion engines. The mobility viewpoint is used here to develop "impedance" vectors, which define the bearing reaction vector in terms of the pure squeeze velocity and bearing position vectors.

The developments of this work are based on the following premises and results:

(*a*) The analytic models presently used in rotordynamic analysis for plain journal bearings (or squeeze-film damper) are inadequate in accuracy and either computational or analytical convenience when compared to existing mobility solutions.

(*b*) The form of mobility descriptions for bearing characteristics is unsuitable for rotordynamic analysis.

(*c*) Impedance descriptions, which are suitable for rotordynamic analysis, can be directly developed from the mobility viewpoint and

[1] This work was supported in part by NASA contract NAS8-31233 administered by the George C. Marshall Space Flight Center, Al. 35812.

[2] Numbers in brackets designate References at end of paper.

Contributed by the Lubrication Division and presented at the Joint Lubrication Conference, Boston, Mass., October 5, 1976, of THE AMERICAN SOCIETY OF MECHANICAL ENGINEERS. Manuscript received by the Lubrication Division March 3, 1976; revised manuscript received June 25, 1976. Paper No. 76-Lub-24.

provide a degree of accuracy and convenience which is equivalent to existing mobility solutions.

(*d*) Alternatively, transformations can be developed between impedance and mobility descriptions which both simplify the numerical calculation of mobility descriptions and mean that any existing mobility description can be converted into an equivalent impedance description for rotordynamics work.

(*e*) Impedance descriptions of bearings (or squeeze-film dampers) provide a dynamic nonlinear definition of a bearings reaction force as a function of its motion. Hence, they are directly applicable for transient simulation work. Further, they are particularly convenient for small motion about an equilibrium position.

Statement (*a*) above is supported by a comparison of bearing models presently used in rotordynamic analysis with existing mobility descriptions. In rotordynamic analysis, the Ocvirk (short) and Sommerfeld (long) bearing models continue to be the most commonly encountered *analytic* bearing descriptions. For example, Kirk and Gunter [5, 6, 7] have recently employed the short bearing model for rotordynamic analysis, while Simandiri and Hahn [8] and Tonneson [9] have used the short-bearing model in the analysis of squeeze-film dampers. Vance and Kirton [10] have examined the appropriateness of the long-bearing model for "long" squeeze-film dampers with end seals. The most commonly used *analytic* finite-length bearing model is that of Warner [11].

From a numerical viewpoint, several investigators have attacked the combined transient bearing-rotordynamic problem by solving the Reynolds equation for the bearing reaction force, while simultaneously integrating the rotor equations of motion. This approach is followed by Kirk and Gunter for the short-bearing model [5, 6, 7] and by Myrick and Rylander [12][3] for finite-length bearings. On the mobility side, Booker [1] developed analytic mobility vectors for the three approximate models cited above (Ocvirk, Sommerfeld, and Warner-Sommerfeld) for both cavitating and noncavitating conditions. Booker accounted for cavitation by setting the pressure equal to zero at locations where it otherwise might have been negative to obtain so-called "π"-bearing mobilities. Blok and his co-workers [4] solved the Reynolds equation directly via finite differences to obtain mobility descriptions for finite-length bearings. The numerically calculated mobilities were based on an improved cavitation model, viz., the circumferential pressure gradient was required to be zero at the leading and trailing edges of cavitation. A comparison of numerically calculated finite-length mobilities with the approximate analytic solutions yielded the following conclusions:

(*a*) For short bearings ($L/D < \frac{1}{2}$), the Ocvirk model gives a reasonably good definition of the bearing-reaction direction but predicts an erroneously large magnitude. The error in the magnitude increases sharply for high eccentricity ratios.

(*b*) The Sommerfeld and Warner-Sommerfeld impedance models provide an improved definition of the bearing reaction magnitude for long bearings ($L/D > 1$) and high eccentricity ratios, but both provide (the same) inaccurate definition of its direction.

Moes and Herrebrugh [13] and Moes [14] subsequently developed analytic expressions which "fitted" the numerically calculated mobility results, and were built up from asymptotic versions of the (analytic) Ocvirk and Sommerfeld solutions. These finite bearing models are quite accurate and are (surprisingly) simpler in form than either the Ocvirk or Sommerfeld π models. Their accuracy has been verified by an exhaustive numerical-experimental study by Campbell, et al. [15]. In summary, the mobility models provide a more accurate and convenient definition of the dynamic-characteristics of plain journal bearings than the models presently employed for rotordynamic analysis.

The impedance method is introduced (in the following section) by directly deriving impedances for the Ocvirk and Sommerfeld bearing models in a manner which parallels Booker's [1] mobility derivation. For cavitating bearings, the result demonstrates that the impedance vector is a more natural definition than the mobility vector in the sense that it can be determined more easily and directly. The magnitudes of the impedance and mobility vectors are shown to be reciprocals. The transformation relationships between these alternative bearing descriptions means that (*a*) the *numerical* calculation of mobilities can be simplified by first calculating impedance vectors and then transforming to obtain the desired mobility vector, and (*b*) impedance vectors that are suitable for rotordynamic analysis can be obtained directly from existing mobility definitions including the finite-length model of Moes [14].

Transient numerical results are presented for short bearing impedances and a finite-length cavitating impedance based on the mobility of reference [14]. Comparisons are made here between the impedance formulations and the direct-integration short-bearing approach of Kirk and Gunter [5–7]. The results of the short-bearing impedance model coincide with the direct-integration formulation, but require about one tenth of the computer time. At large eccentricities, the predicted orbits are larger for the finite-length impedance than the short-bearing impedance. Transient simulation results are also presented and compared with Tonneson's [9] experimental results for short squeeze-film dampers.

While a nonlinear impedance description is attractive for transient rotordynamic analysis, historically, the bulk of bearing analysis for rotordynamics has been concerned with the calculation of linear stiffness and damping coefficients for small motion about an equilibrium point. Lund and Sternlicht [17] initially calculated such coefficients by numerical differentiation of a finite difference solution to the Reynolds equation. Orcutt and Arwas [18] used a similar

[3] Myrick and Rylander include the effect of a change in slope of the rotor at the bearing, which is not allowed with the mobility or impedance formulations.

Nomenclature

a = magnitude of rotor imbalance, L
C = radial clearance, L
D = bearing diameter, L
$\mathbf{F}$ = bearing reaction force (the force applied to the journal from the fluid film), F
$\mathbf{F}_L$ = bearing load force (the force applied from the journal to the fluid film; $F = -F_L$), F
g = gravitational constant, LT^{-2}
h = normalized film thickness
$\mathbf{I}, \mathbf{J}, \mathbf{K}$ = unit vectors in X, Y, Z system
J = rotor polar moment of inertia, FLT^2
L = bearing length, L
$\mathbf{M}$ = mobility vector
m = rotor mass, FT^2L^{-1}
p = film pressure, FL^{-2}
P = mean film pressure (axially), FL^{-2}
R = bearing radius, L
S = Sommerfeld number, $S = F_0(\mathrm{C/R})^2/2\mu\bar{\omega}LD$
T_ϕ = applied torque to rotor, FL
$\mathbf{u}_\epsilon$, u_β = unit vectors along and normal to ϵ
$\mathbf{V}$ = journal center velocity relative to the X, Y, Z system, LT^{-1}
$\mathbf{V}_s$ = pure-squeeze journal velocity relative to the X, Y, Z system, LT^{-1}
$\mathbf{W}$ = impedance vector
X, Y, Z = stationary coordinate system which is inertial for rotordynamics work
x, y, z = V_s-fixed coordinate system
x', y', z' = $\mathbf{F}$-fixed coordinate system
α = attitude angle of ϵ relative to $\mathbf{V}_s$
β = attitude angle of ϵ relative to $\mathbf{I}$
γ = attitude angle of ϵ relative to $\mathbf{F}$
ϵ = eccentricity-ratio vector
ζ = attitude angle of $\mathbf{V}_s$ relative to $\mathbf{I}$
θ = bearing polar cylindrical coordinates with respect to-ϵ
μ = lubricant viscosity, $FL^{-2}T$
ϕ = rotor rotation angle
ψ = attitude angle of $\mathbf{W}$ relative to $\mathbf{V}_s$
$\omega_{s,j}$ = angular velocity of the sleeve (journal) about the Z-axis, T^{-1}
$\bar{\omega}$ = average of ω_j *and* ω_s, T^{-1}
$[a]$ = matrix of stiffness coefficients, FL^{-1}
$[b]$ = matrix of damping coefficients, FTL^{-1}

Subscripts

0 = denotes equilibrium position
ϵ = vector component in u_ϵ direction
β = vector component in u_β direction

analysis approach to obtain stiffness and damping coefficients for both laminar and turbulent conditions. Reinhoudt [18] also employed the numerical differentiation approach for obtaining bearing coefficients, but solved the Reynolds equation with a finite-element approach. Lund [19] has developed a pertubation solution approach to the Reynolds equation, which eliminates the requirement of numerical differentiation.

Analytic solutions for stiffness and damping coefficients have been defined for the short-bearing model [6], but the deficiencies of this model have been previously noted. An attractive solution to this problem has been provided by Moes [20], who obtained the desired analytic coefficient definitions by (analytic) partial differentiation of the mobility vector. A comparable derivation of (analytic) stiffness and damping coefficients from an impedance vector definition is given here, and results are presented for a cavitating finite-length-bearing impedance based on [14]. The resulting coefficients are shown to generally agree with those of Orcutt and Arwas [17], and Reinhoudt [18], and are used for linear stability analysis of a rigid rotor, which is symmetrically supported by plain journal bearings. Onset-speed-of-instability results are presented for a range of bearing numbers as a function of the L/D ratio.

The Ocvirk (Short) and Sommerfeld (Long) Impedances

The Reynolds equation for a constant-viscosity incompressible fluid can be stated in polar-cylindrical coordinates as

$$\frac{\partial}{\partial\theta}\left(h^3\frac{\partial p}{\partial\theta}\right)+R^2\frac{\partial}{\partial Z}\left(h^3\frac{\partial p}{\partial Z}\right)=\frac{12\mu R^2}{C^3}\{C\dot{\epsilon}c\theta+C\epsilon(\dot{\beta}-\bar{\omega})s\theta\} \quad (1)$$

where h is the normalized film thickness defined by

$$h=1+\epsilon c\theta, \quad (2)$$

$s\theta=\sin\theta$, $c\theta=\cos\theta$, Z is the axial position variable, and the kinematic variables ϵ, β, θ are illustrated in Fig. 1. Further, μ and p are the fluid viscosity and pressure, respectively, and C and R are the journal clearance and radius, respectively. The variable $\bar{\omega}$ is the half angular velocity of the journal about the Z axis, relative to the stationary X, Y, Z system.[4]

The physical interpretation provided by Booker and Blok for the terms on the right hand side of equation (1) contributes significantly to an appreciation of the development of either mobility or impedance vectors, and goes as follows. The velocity of the journal center relative to the stationary X, Y, Z system is

$$\mathbf{V}=\left.\frac{dC\epsilon}{dt}\right|_{X,Y,Z}$$

We denote the time rate of change of the vector $C\epsilon$ with respect to a coordinate system that has an angular velocity of $\bar{\omega}\mathbf{K}$ relative to the stationary X, Y, Z coordinate system by $\mathbf{V}_s$ and observe the following relationship

$$\mathbf{V}_s=\mathbf{V}-\mathbf{K}\bar{\omega}\times C\epsilon=\mathbf{u}_\epsilon C\dot{\epsilon}+\mathbf{u}_\beta C\epsilon(\dot{\beta}-\bar{\omega}) \quad (3)$$

Hence, the terms $C\dot{\epsilon}$, $C\epsilon(\dot{\beta}-\bar{\omega})$ of equation (1) are the velocity components of the journal center with respect to a coordinate system that is rotating at an angular velocity of $\mathbf{K}\bar{\omega}$ relative to the stationary X, Y, Z system. Booker and Blok note that the journal center's motion from this type of rotating coordinate system would always appear to be in a state of pure squeezing. Hence the vector $\mathbf{V}_s$ is denoted here as the journal's pure-squeeze-velocity vector.

Given that the velocity and position of the journal center relative to the stationary coordinate system are defined by

$$C\epsilon=\mathbf{I}X+\mathbf{J}Y=C\epsilon(\mathbf{I}c\beta+\mathbf{J}s\beta)$$

$$\mathbf{V}=\mathbf{I}\dot{X}+\mathbf{J}\dot{Y}=\mathbf{u}_\epsilon C\dot{\epsilon}+\mathbf{u}_\beta C\epsilon\dot{\beta}, \quad (4)$$

the pure squeeze-velocity vector is defined in the stationary X, Y, Z system by

$$\mathbf{V}_s=\mathbf{V}-(\mathbf{K}\bar{\omega}\times C\epsilon)=\mathbf{I}(\dot{X}+\bar{\omega}Y)+\mathbf{J}(\dot{Y}-\bar{\omega}X) \quad (5)$$

Alternatively, from fig. 2,

$$\mathbf{V}_s=V_s(\mathbf{u}_\epsilon c\alpha-\mathbf{u}_\beta s\alpha)=V_s(\mathbf{I}c\zeta+\mathbf{J}s\zeta)$$

Substitition from this result and equation (3) yields the following restatement of the Reynolds equation (1)

$$\frac{\partial}{\partial\theta}\left(h^3\frac{\partial p}{\partial\theta}\right)+R^2\frac{\partial}{\partial Z}\left(h^3\frac{\partial p}{\partial Z}\right)=\frac{12\mu R^2V_s}{C^3}c(\alpha+\theta) \quad (6)$$

Ocvirk (Short) Bearing Solution. The Ocvirk solution to equation (6) is obtained by neglecting the first term on the left, and solving for $p(\theta, Z)$ with the boundary conditions $p(\theta, L/2)=p(\theta, -L/2)=0$, to obtain

$$p(\theta,Z)=-3\mu L^2(1-(2Z/L)^2)V_sc(\alpha+\theta)/2C^3h^3 \quad (7)$$

Integrating axially yields the following average pressure definition

$$P(\theta)=\frac{1}{L}\int_{\frac{L}{2}}^{\frac{L}{2}}p(\theta,Z)\,dZ=-\mu L^2V_sc(\alpha+\theta)/C^3h^3 \quad (8)$$

The pressure is seen to be positive between the angles θ_1, θ_2 defined by

$$\theta_1=\frac{\pi}{2}-\alpha, \qquad \theta_2=\frac{3\pi}{2}-\alpha \quad (9)$$

In words, the pressure is positive over a region of π radians centered about $\mathbf{V}_s$.

Sommerfeld (Long) Bearing Solution. The Sommerfeld solution to the Reynolds equation is obtained by dropping the second term

[4] If the sleeve also rotates, $\bar{\omega}$ is the average of the sleeve and journal angular velocities, i.e., $\bar{\omega}=(\omega_s+\omega_j)/2$.

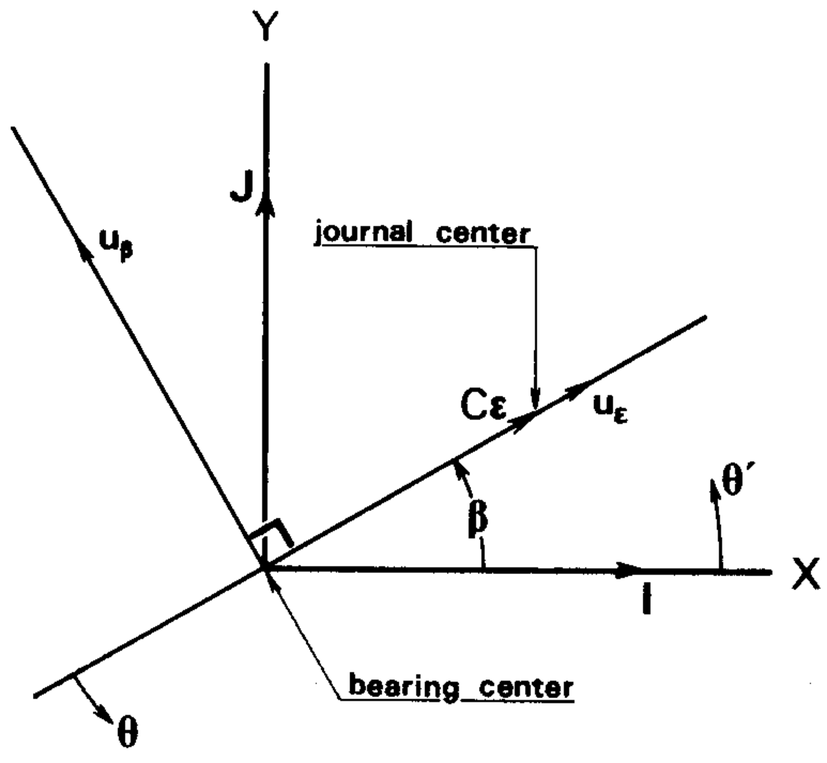

Fig. 1 Plain journal bearing kinematic variables

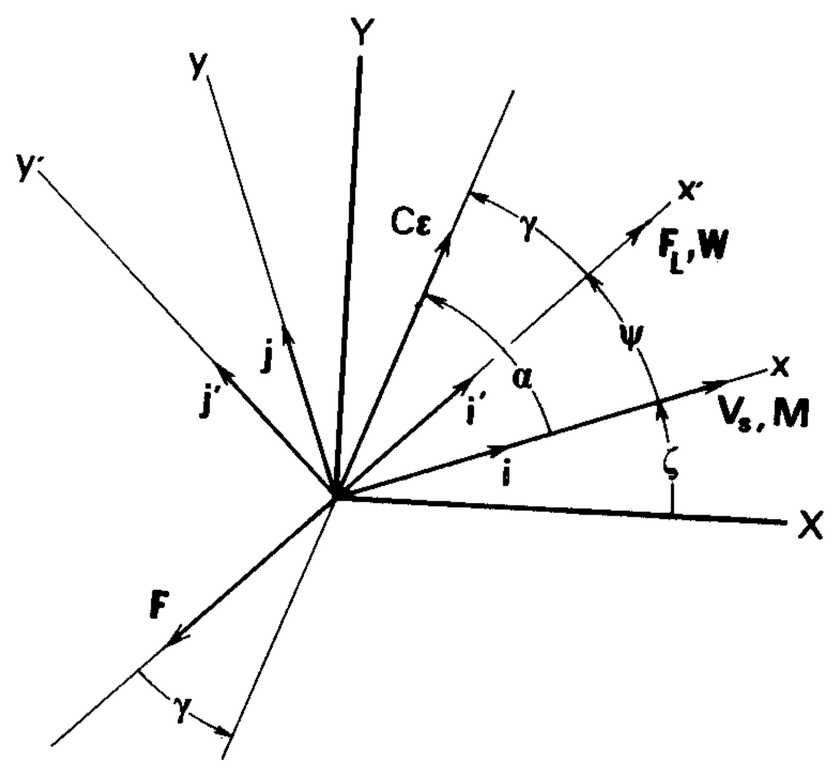

Fig. 2 Kinematic variables for impedances and mobilities

on the left in equation (6) and integrating with respect to θ to obtain

$$P(\theta) = -6\mu R^2 V_s(c\alpha c\theta - bs\alpha s\theta)(2 + \epsilon c\theta)/C^3h^2 \tag{10}$$

where

$$b = 2/(2 + \epsilon^2) \tag{11}$$

From equation (10) the positive pressure sector lies between the angles θ_1, θ_2 defined by

$$b\ tg\theta_1 = (tg\alpha)^{-1}, \qquad \theta_2 = \theta_1 + \pi \tag{12}$$

This solution is taken from Booker [1], who credits it to Gross [21]. The Warner-Sommerfeld solution [11] differs from this solution by the factor $\Pi(\alpha, \epsilon)$ which accounts for end-leakage [1]. However, both the Sommerfeld and Warner-Sommerfeld solutions yield the same direction for the bearing reaction force. The boundary conditions used to obtain equation (10) are (a) periodicity with respect to θ, i.e., $P(\theta) = P(\theta + 2\pi)$, and ($b$) the requirement that the positive pressure sector extends over π radians, i.e., $P(\theta_1) = P(\theta_1 + \pi) = 0$.

Impedance Definitions. The forces acting on the journal can be obtained by integrating these pressure distributions. A complete film "2π" bearing is obtained by integrating over $[0, 2\pi]$, while a ruptured-film "π" bearing is obtained by integrating only the positive portion of the film, i.e., $[\theta_1, \theta_2]$. The π bearing provides an approximate model for cavitation, since the assumption is made that film rupture prevents the development of negative pressures, and tends to be the more generally applicable model.

Integration of the pressure distribution from the preceding section yields the following definition for the force components parallel and normal to the eccentricity vector

$$F_\epsilon = RL\int P(\theta)c\theta d\theta$$
$$F_\beta = RL\int P(\theta)s\theta d\theta \tag{13}$$

which can be stated

$$F_\epsilon = -V_s 2\mu L(\mathrm{R/C})^3 W_\epsilon(\alpha, \epsilon)$$
$$F_\beta = -V_s 2\mu L(R/C)^3 W_\beta(\alpha, \epsilon) \tag{14}$$

The quantities W_ϵ, W_β are the desired components of the impedance vector **W**, whose vector character is emphasized by the following restatement of equation (14)

$$\mathbf{u}_\epsilon F_\epsilon + \mathbf{u}_\beta F_\beta = -V_s 2\mu \mathrm{L}(R/C)^3(\mathbf{u}_\epsilon W_\epsilon + \mathbf{u}_\beta \mathrm{W}_\beta) \tag{15}$$

For computational purposes, the following definition of **W** in terms of its components parallel and normal to the squeeze-velocity vectors $\mathbf{V}_s$ is convenient.

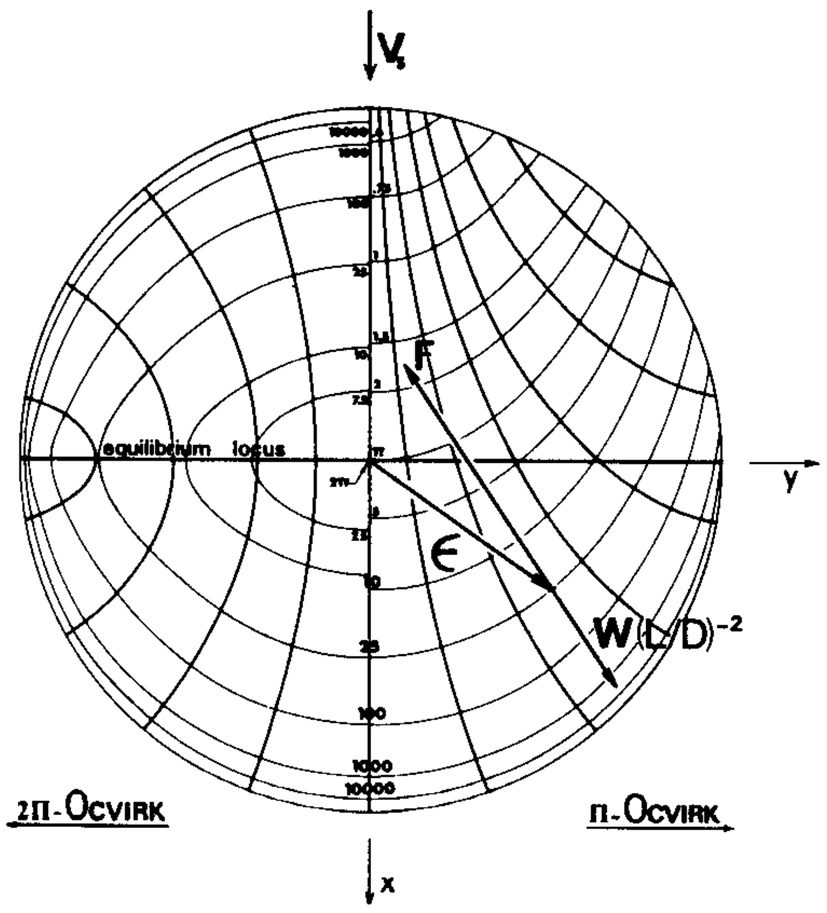

Fig. 3 Impedance plot for the Ocvirk (short) π and 2π bearing model

$$W_x = W_\epsilon c\alpha - W_\beta s\alpha$$
$$W_y = W_\epsilon s\alpha + W_\beta c\alpha \tag{16}$$

Fig. 3 illustrates the impedance plot for the Ocvirk π and 2π solutions, respectively, in terms of these components. A similar definition of the components of **W** in the X, Y system is readily stated in terms of the angle β.

The impedance descriptions for the Ocvirk (short) bearing model are obtained by substitution from equation (8) into equations (13) and (14) to obtain

$$W_\epsilon = 2(J_3{}^{02}c\alpha - J_3{}^{11}s\alpha)(L/D)^2$$
$$W_\beta = 2(J_3{}^{11}c\alpha - J_3{}^{20}s\alpha)(L/D)^2 \tag{17}$$

where[5]

$$J_m{}^{jk} = \int s^j\theta c^k\theta h^{-m}d\theta \tag{18}$$

The solution for both the π and 2π bearings are defined by this relationship. They differ only in bounds of integration used, viz., $[0, 2\pi]$ for the 2π bearing and $[\theta_1, \theta_2]$ for the π bearings. Hence, for the π bearing the integrals are a function of both α and ϵ, while for the 2π bearing, they depend only on ϵ. For small ϵ, the π bearing impedance reduces to

$$W_x = 2(\pi/2 + 4\epsilon c\alpha)(L/D)^2$$
$$W_y = 2(2\epsilon s\alpha)(L/D)^2 \tag{19}$$

For the Sommerfield (long) bearing, the following impedance components are obtained by substitution from equation (10) into equations (13) and (14).

$$W_\epsilon = 3(B_{11}c\alpha - bB_{21}s\alpha)$$
$$W_\beta = 3(B_{21}c\alpha - B_{22}s\alpha) \tag{20}$$

where

$$B_{11} = 2J_2{}^{02} + \epsilon J_2{}^{03}, \qquad B_{21} = 2J_2{}^{11} + \epsilon J_2{}^{12}$$
$$B_{22} = b(2J_2{}^{20} + \epsilon J_2{}^{21}) \tag{21}$$

As with the short-bearing solution, both the π and 2π impedance vectors are defined by these results, and differ only in the integration bounds used to evaluate the integrals of equation (21). For small ϵ, the π bearing solution reduces to

$$W_x = 3(\pi + 4\epsilon c\alpha), \qquad W_y = 3(2\epsilon s\alpha) \tag{22}$$

which resembles the short-bearing result of equation (19).

The statement was made in the introduction that (for cavitating conditions) the impedance vector definition is more easily obtained than a mobility vector. The explanation of this statement goes as follows. With cavitation, the integrals of equation (18) must be defined in terms of the limits (θ_1, θ_2) which are a function of α. In calculating the impedance vector, $\mathbf{V}_s$ is known which defines α, and allows one to directly calculate **W** and hence the reaction force **F**. In calculating a mobility vector the reaction force is assumed to be the negative of the applied force, and is given; however, $\mathbf{V}_s$ and hence α are unknown. For a *given* **F**, one must accordingly iterate to find α. The relationships between mobility and impedance vectors are discussed in the following section.

Relationships Between Mobility And Impedance Vectors

As noted in the introduction, mobilities were developed to address the following problem. Given a force $\mathbf{F}_L$ applied from the journal to the fluid film and the position of the journal, determine its instantaneous velocity and subsequent motion. In rotordynamics we are considering a *related but distinctly different problem;* viz., given the

[5] Booker [27] provides a convenient summary of these integrals; however, for the present work, the following definition for $J_1{}^{00}$ was employed

$$J_1{}^{00} = 2(1 - \epsilon^2)^{-1/2}\left[n\pi + tg^{-1}(1 - \epsilon)^{1/2}(1 + \epsilon)^{-1/2}tg\left(\frac{\theta}{2}\right)\right]$$
$$(2n - 1)\pi \leqslant \theta \leqslant (2n + 1)\pi$$

position and velocity of the journal, determine the bearing reaction force **F** (the force acting from the fluid film on the journal). Obviously, $\mathbf{F} = -\mathbf{F}_L$.

The mobility approach is most readily applicable for bearings of internal combustion engines for which the applied load $\mathbf{F}_{ap}$ is known and dominant in comparison to the inertia effects of the rotor, and *under these circumstances* $\mathbf{F}_L \simeq \mathbf{F}_{ap}$. In rotordynamic situations, however, the stiffness and inertia properties of the rotor must be accounted for, and the desired and most easily calculated force is the bearing reaction force **F**. Impedances have accordingly been derived (here) in terms of **F**, not $\mathbf{F}_L$, and readers with a historical perspective of impedances are urged to note this distinction in reviewing the following material.

Booker [1] introduced the following definition for the mobility vector

$$\mathbf{M} = \frac{R^3}{C^3}\frac{2\mu L}{F_L}\mathbf{V}_s = \frac{R^3}{C^3}\frac{2\mu L}{F}\mathbf{V}_s \tag{23}$$

whereas, the impedance vector is defined in equation (14) by

$$\mathbf{W} = -\frac{C^3}{R^3}\frac{1}{2\mu L V_s}\mathbf{F} = \frac{C^3}{R^3}\frac{1}{2\mu L V_s}\mathbf{F}_L \tag{24}$$

From these definitions the magnitudes of **M** and **W** are related by

$$W = M^{-1} \tag{25}$$

As illustrated in Fig. 2, γ defines the orientation of $C\epsilon$ relative to **W**, and is related to α by either of the following relationships

$$tg\alpha = -\frac{M_\beta(\epsilon, \gamma)}{M_\epsilon(\epsilon, \gamma)}, \qquad \mathrm{tg}\gamma = -\frac{\mathrm{W}_\beta(\epsilon, \alpha)}{\mathrm{W}_\epsilon(\epsilon, \alpha)} \tag{26}$$

Transformation from a mobility definition into an impedance definition (or vice versa) can be carried out via equations (25) and (26), and Appendix A contains several impedance definitions which have been derived from previously developed mobility descriptions. Specifically, Appendix A contains impedances which were obtained via equations (25) and (26) for small and large eccentricity approximations to the π Ocvirk and π Sommerfeld solutions first stated by Booker [1]. These asymptotic solutions are used in the following section in the derivation of a finite-length impedance comparable to the finite-length mobility of reference [14].

The transformation relationship of equations (26) is a polar representation for the $\mathbf{u}_\epsilon$, $\mathbf{u}_\beta$ eccentricity-vector-oriented unit vector system, and is essential for analytic transformations. From Fig. 2, the following cartesian transformations for the components of $\boldsymbol{\epsilon}$ are useful in numerical transformations between mobility and impedance vectors.

$$\begin{aligned} \epsilon_{x'} &= (\epsilon_x W_x + \epsilon_y W_y)/W \\ \epsilon_{y'} &= (-\epsilon_x W_y + \epsilon_y W_x)/W \end{aligned} \tag{27}$$

$$\begin{aligned} \epsilon_x &= (\epsilon_{x'} M_{x'} - \epsilon_{y'} M_{y'})/M \\ \epsilon_y &= (\epsilon_{x'} M_{y'} + \epsilon_{y'} M_{x'})/M \end{aligned} \tag{28}$$

To illustrate the use of these relationships, suppose one has an impedance definition in terms of the components $W_x(\epsilon_x, \epsilon_y)$, $W_y(\epsilon_x, \epsilon_y)$. The magnitude of the associated mobility vector is defined by equation (25), and its position (relative to the **F**-oriented x', y' system) is defined by equation (27).

Finite Bearing Impedance Descriptions

A considerable amount of information about mobilities is available in the publications of Booker [1, 2, 3], Blok [4] and Moes [13, 14, 20], concerning topological aspects as well as numerical and graphical data. This information is the basis for the finite-length bearing impedances developed here.

The following two *asymptotic* solutions for plain journal bearings have proven to be useful in the mobility analysis of transient bearing phenomena:

(a) the Ocvirk (short) bearing solution for small eccentricity ratios, and

(b) the Sommerfeld (long) bearing solution for large eccentricity ratios. Impedance definitions are provided in Appendix A for these asymptotic solutions. Individually, these asymptotic solutions have a limited value which is consistent with their restricted range of application in both L/D (length to diameter) and eccentricity ratios. Fortunately, the fact that their ranges of application do not coincide means that the two (vector) solutions can be combined in such a way that an approximate solution is obtained which is valid for general finite-length bearings at both large and small eccentricity ratios.

As noted in the introduction, this method has been used in the development of analytic definitions for finite-length mobilities, and is based on the observed fact that a vectorial sum of the Ocvirk and Sommerfeld mobilities provides an excellent approximation for the actual (numeric) mobility vector for all eccentricity and L/D ratios. Hence, Moes [14] used a weighted sum of the asymptotic solutions cited above to obtain a finite-length analytic mobility vector, which has the same order of accuracy as the numeric mobility data on which it is based.

This technique is used here to directly derive 2π and π finite-length impedance descriptions. The 2π impedance description is given as solution 5 in Appendix A; however, the π impedance vector is used in subsequent transient simulations and will be reviewed here. We require a definition of the vector **W** and propose to obtain W and γ in terms of ϵ and α. The variables ϵ, α, γ are related through equations (26) by the transcendental equation

$$tg(\gamma - \alpha) = \frac{3}{4}\frac{\epsilon s\gamma}{(1 - \epsilon c\gamma)}\frac{(1 + 3.60A)}{(1 + 2.12A)}, \qquad A = (1 - \epsilon c\gamma)(L/D)^{-2},$$

which fortunately has the excellent approximate solution

$$\gamma \cong \{1 - \xi'(1 - \eta'^2)^{-1/2}\}\left[tg^{-1}\left\{\frac{4(1 + 2.12B)(1 - \eta'^2)^{1/2}}{3(1 + 3.60B)\eta'}\right\} - \frac{\pi}{2}\eta'/|\eta'| + s^{-1}\eta'\right] + \alpha - s^{-1}\eta' \tag{29}$$

$$B = (1 - \epsilon^2)(L/D)^{-2}$$

where

$$\xi' = \epsilon c\alpha, \qquad \eta' = \epsilon s\alpha \tag{30}$$

The amplitude W can now be expressed

$$\left.\begin{aligned} W &= \{0.150(E^2 + G^2)^{1/2}(1 - \xi)^{3/2}\}^{-1} \\ E &= 1 + 2.12Q, \qquad \mathrm{G} = 3\eta(1 + 3.60Q)/4(1 - \xi) \\ Q &= (1 - \xi)(L/D)^{-2} \end{aligned}\right\} \tag{31}$$

where

$$\xi = \epsilon c\gamma, \qquad \eta = \epsilon s\gamma \tag{32}$$

From Fig. 2, the impedance components parallel and perpendicular to the squeeze-velocity $\mathbf{V}_s$ are

$$W_x = Wc\psi, \qquad W_y = Ws\psi, \qquad \psi = \alpha - \gamma \tag{33}$$

Rotordynamic Simulation Examples Using Impedance Vectors

In this section, transient rotor simulations will be demonstrated which illustrate the impedance procedure for modeling a plain journal bearing. The following simplified rigid-body horizontal-rotor model is to be used.

$$\begin{aligned} m\ddot{X} &= F_X + m(a_X\dot{\phi}^2 + a_Y\ddot{\phi}) \\ m\ddot{Y} &= F_Y + m(a_Y\dot{\phi}^2 - a_X\ddot{\phi}) - mg \\ a_X &= ac\phi, \qquad a_Y = as\phi \\ J\ddot{\phi} &= T_\phi \end{aligned} \tag{34}$$

where g is the acceleration of gravity, and the parameters m, J, a are the rotor's mass, polar moment of inertia, and imbalance-vector magnitude, respectively. The position of the rotor is defined in the

stationary coordinate system of Fig. 1 by X, Y, and the rotor's rotation (not precession) is defined by the angle ϕ; hence, $\bar{\omega} = \dot{\phi}/2$. The torque applied to the rotor is T_ϕ, and the components of the external force acting on the rotor are F_X, F_Y. For our present purposes, the external forces considered are bearing forces only.

The basic problem in modeling a bearing is the definition of the reaction force components as a function of the position (X, Y) and velocity vector components ($\dot{X}$, $\dot{Y}$), and the spin velocity $\dot{\phi}$. The solution to this problem for the short and long bearing impedances is summarized in the following steps:

(a) From equation (4) one calculates

$$\epsilon = (X^2 + Y^2)^{1/2}/C$$

The 2π bearing integrals can now be calculated.

(b) From equations (4) and (5) and Fig. 2

$$s\beta = Y/C\epsilon, \qquad c\beta = X/C\epsilon$$

$$s\zeta = (\dot{Y} + \bar{\omega}X)/V_s, \qquad c\zeta = (\dot{X} - \bar{\omega}Y)/V_s, \qquad \bar{\omega} = \dot{\phi}/2$$

$$s\alpha = s(\beta - \zeta) = s\beta c\zeta - c\beta s\zeta$$

$$c\alpha = c(\beta - \zeta) = c\beta c\zeta + s\beta s\zeta$$

The short and long π bearing integrals can now be evaluated in terms of ϵ, $s\alpha$, $c\alpha$.

(c) The short and long bearing impedances can be evaluated in terms of the W_ϵ, W_β components definitions of equations (17) and (20), respectively. The reaction force components F_ϵ, F_β are then defined by equation (14), and the stationary reaction components are defined via the coordinate transformation

$$F_X = F_\epsilon c\beta - F_\beta s\beta, \qquad F_Y = F_\epsilon s\beta + F_\beta c\beta \tag{35}$$

Alternatively, the transformation relationship of equation (16) can be used to obtain (explicitly) the impedance definition $W_x(\alpha, \epsilon)$, $W_y(\alpha, \epsilon)$ in the "squeeze-velocity-vector" oriented x, y system, which yields

$$F_X = F_x c\zeta - F_y s\zeta, \qquad F_Y = F_x s\zeta + F_y c\zeta \tag{36}$$

The small ϵ definitions of equations (19) and (22) were used in this study for $\epsilon < 0.01$ to avoid numerical difficulties arising with $J_1{}^{00}$.

The procedure for using the finite-length impedance description of the preceding section involves the definition of ϵ, β, ζ, and α as outlined in steps (a) and (b) above. Equation (30) is then used to define ξ', η' which are in turn used to calculate γ in equation (29). Similarly, ξ, η are calculated from equation (32), and then used to calculate the impedance magnitude W from equation (31). Finally, the impedance components of equation (33) are used to calculate the reaction components F_x, F_y, and equation (36) yields the desired stationary-coordinate reaction definition. The finite-length impedance of the preceding section is well behaved for small ϵ and does not require a separate "small ϵ" definition comparable to equations (19) and (22) for the π Ocvirk and Sommerfeld impedances.

The short-bearing formulation proposed by Kirk and Gunter for rotordynamic applications uses the following integral force definition

$$\mathbf{F} = -\mu R L^3 \int \{(\dot{X} + \bar{\omega}Y)c\theta' + (\dot{Y} - \bar{\omega}X)s\theta'\} H^{-3}\mathbf{u}\, d\theta' \tag{37}$$

where θ' is measured from the X axis as illustrated in Fig. 1, and

$$\mathbf{F} = \mathbf{I}F_X + \mathbf{J}F_Y, \qquad \mathbf{u} = \mathbf{I}c\theta' + \mathbf{J}s\theta'$$

$$H = C - Xc\theta' - Ys\theta'$$

The integration in equation (37) is to be performed numerically, and cavitation is accounted for by setting the integrand to zero at locations where it would otherwise be negative.

Numerical integration here was performed with the Newton-Cotes quadrature formula recommended by Kirk and Gunter [5] with a stepsize of $\pi/30$ radians.

It is worth noting that the components of $\mathbf{V}_s$ appear explicitly in equation (37), i.e., $V_{sX} = \dot{X} + \bar{\omega}Y$; $V_{sY} = \dot{Y} - \bar{\omega}X$. Hence, an alternative derivation of the short-bearing impedance description is easily

Table 1 Physical and computational data for transient numerical solutions; all data in SI units; NS = number of integration steps; ΔT = integration stepsize.

Case	m	a	ΔT	NS	$\dot{\phi}$ (rad/s)
1	816.5	0	$2. \times 10^{-4}$	231	680
2	22.68	2.54×10^{-5}	$1. \times 10^{-4}$	287	1100

$C = 127 \times 10^{-4}$, $R = L = 2.54 \times 10^{-2}$, $\mu = 6.897 \times 10^{-2}$

obtained from equation (37) with the coordinate transformation of equation (36) and the geometric relationship between α, β, ζ, θ and θ' illustrated in Figs. 1 and 2.

Transient solutions are obtained by numerical integration of equation (34). The two cases summarized in Table 1 were selected from reference [7] and solved using (a) the Ocvirk impedance formulation, (b) the numeric integral formulation of equation (37), and (c) the finite-length impedance description of the preceding section. All cases are for constant spin velocity ($T_\phi = 0$). The initial conditions for case 1 are $\phi = X = \dot{X} = Y = \dot{Y} = 0$, $\dot{\phi} = 680$ rad/s (6500 rpm). The initial conditions for case 2 were obtained by integrating the model for approximately ten revolutions from the initial conditions $\phi = X = Y = \dot{X} = \dot{Y} = 0$, $\dot{\phi} = 1100$ rad/s (10500 rpm).

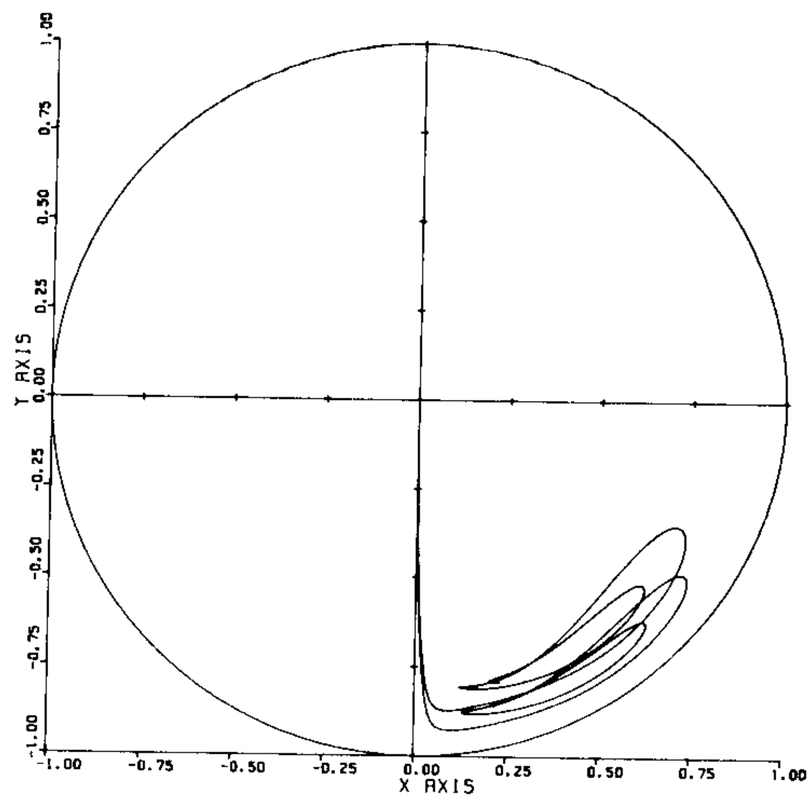

Fig. 4(a) Transient solution to case 1 (Table 1) from (a) the Ocvirk impedance and the stationary integral formulation of equation (37), and (b) the finite-length impedance of equations (29)–(32)

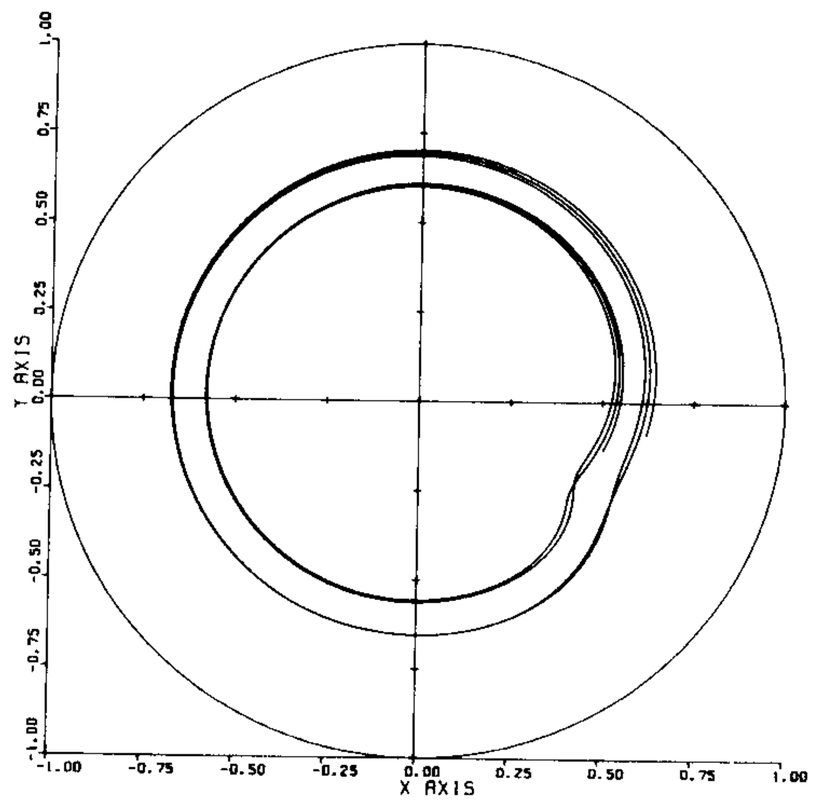

Fig. 4(b) Transient solution to case 2 (Table 1) from (a) the Ocvirk impedance and the stationary integral formulation of equation (37), and (b) the finite-length impedance of equations (29)–(32)

The solutions for these cases with the Ocvirk impedance and the numerical integration formulations of equation (37) basically coincide, but yield orbits which are too small (or clearances which are too large) when compared to the finite-length impedance results. The solutions are illustrated in Fig. 4 for approximately five rotor revolutions. These results would be expected since the $L/D = ½$ ratio is near the valid range of short-bearing model, particularly at eccentricity ratios in excess of 0.5.

On a normalized basis, the computer time requirements for (a) the Ocvirk impedance formulations, (b) the finite-length impedance formulations of equations (29)–(32), and (c) the direct numerical integration form of equation (37) are approximately 1:1.67:10.5. These ratios are based on a number of numerical cases in addition to the solutions presented in Fig. 5 and emphasize the advantages of the impedance formulation for the transient solution of plain journal bearings.

As noted previously, the applicability of the impedance formulation is restricted to bearings which can be defined by a mobility vector. This generally means that the bearing must have circumferential symmetry, and many bearings fail to meet this criterion; however, most squeeze-film dampers are circumferentially symmetric, and can be modeled by impedances. Tonneson has recently reported [9] the results of an experimental parametric study of squeeze-film dampers, which compared predicted stiffness and damping coefficients with experimentally measured impedances. He found the correlation between theory and measurement to be excellent for concentric cases, but concluded that the motion at large eccentricity ratios was basically a nonlinear phenomenon, which was not appropriately modeled by linear stiffness and damping coefficients. A comparison will now be considered between the nonlinear numerically predicted motion from impedances with Tonneson's experimental results.

Tonneson's experimental arrangement causes a mass, which is spring supported in a squeeze-film damper, to be excited by a rotating imbalance. The spring prevents the mass from rotating, and the appropriate differential equation model is

$$m\ddot{X} + kX = F_X + m_1 a\Omega^2 c(\Omega t + \eta_0)$$
$$m\ddot{Y} + kY = F_Y + m_1 a\Omega^2 s(\Omega t + \eta_0) \qquad (38)$$

where m_1a is the rotating imbalance, k is the spring constant, Ω is the imbalance frequency, η_0 is an initial phase angle, and F_X and F_Y define the components of the external force. The orbits of Fig. 5 are taken from Tonneson's work [9].

An analysis of Tonneson's data indicates that there is comparatively little cavitation for the small orbits of Fig. 7, but there is considerable cavitation for the larger orbits. Hence, a cavitating impedance is appropriate for the large orbits and a noncavitating 2π model should be employed for the small orbits. Figs. 6 and 7 illustrate transient simulation results, respectively, for the π Ocvirk and finite-length cavitating impedance description of equations (29)–(32).

The finite-length impedance predicts slightly smaller minimum clearances in the upper plates of these figures, than does the π Ocvirk impedance, but otherwise generally yields the same results. Given the shortness of the damper ($L/D = 0.17$) this agreement between the two impedances would be expected. The impedance results differ from the experimental results of Fig. 5 in the following two important regards:

(a) They generally predict smaller orbit amplitudes than the experimental data.

(b) As the experimental orbit radii decrease, the orbit centers approach the nominal eccentricity condition $\epsilon = 0.75$. This characteristic is much less evident in the impedance results.

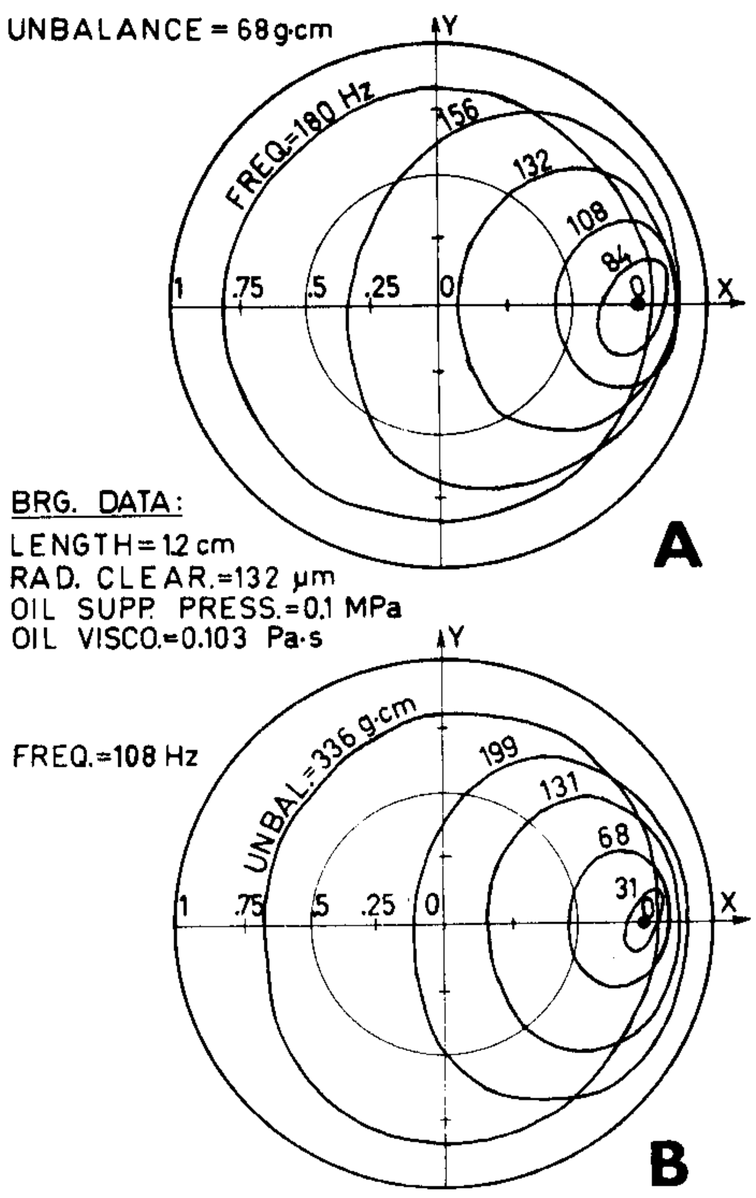

Fig. 5 Tonneson's transient experimental results [9] for a short ($L/D = .17$) squeeze-film damper, nominal eccentricity ratio = 0.75, nominal symmetric support stiffness, $k = 10^7$ N/m

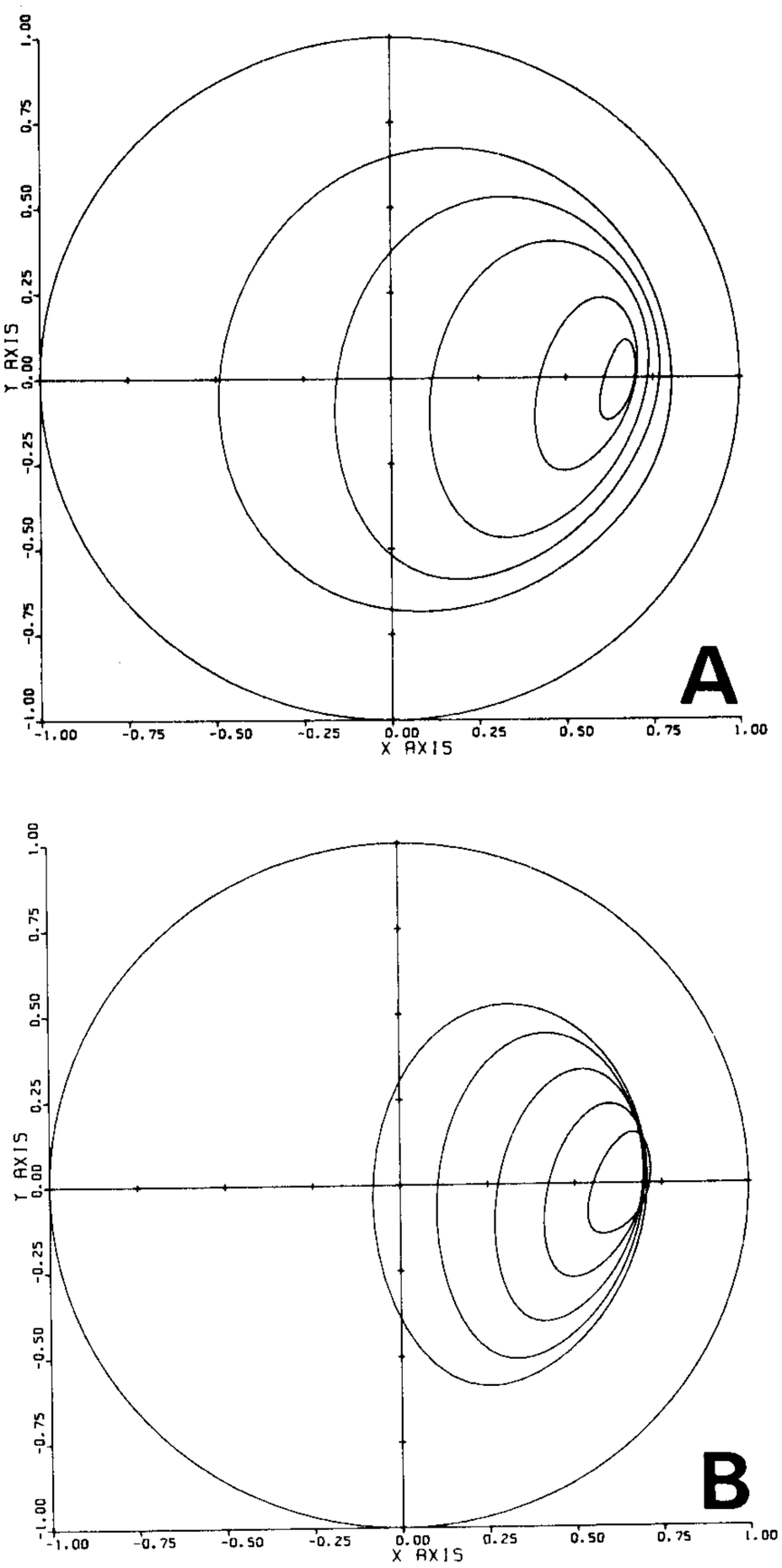

Fig. 6 Transient simulation results using the π Ocvirk impedance model for comparison with Tonneson's experimental results (Fig. 5)

Fig. 8 illustrates the predicted orbits for the 2π Ocvirk impedances, and provides an explanation for point (b). We noted earlier that Tonneson's data show minimal cavitation associated with the smaller orbits. Hence, the 2π model should be better for these cases, and Fig. 8 shows that without cavitation, all of the orbits are centered about $\epsilon = 0.75$. However, the orbit magnitudes are even smaller for the 2π impedance then for the cavitating impedances of Figs. 6 and 7. At present, the authors have no explanation for the erroneously small orbits predicted by the simulation results (other than lubricant starvation).

The point is emphasized that the applicability of the impedance formulation is not restricted to the simple rotor models of equations (34) or (38), and can be readily employed in more general flexible-rotor formulations [22]–[24].

Stiffness and Damping Constants From Impedance Solutions

From a rotordynamic viewpoint, the calculation of stiffness and damping coefficients for bearings and squeeze-film dampers is of comparable or greater importance than the development of nonlinear representations for transient analysis. Stiffness and damping coefficients are customarily required for both synchronous response calculations and linear stability analysis. In this section, we consider the development of linear stiffness and damping coefficients from impedance vectors for small motion about an equilibrium position. The desired coefficients yield the following customary definition for the bearing force

$$\begin{Bmatrix} F_X \\ F_Y \end{Bmatrix} = -[a_{I,J}] \begin{Bmatrix} X \\ Y \end{Bmatrix} - [b_{I,J}] \begin{Bmatrix} \dot{X} \\ \dot{Y} \end{Bmatrix} \tag{39}$$

where $[a_{I,J}]$ and $[b_{I,J}]$ are matrices of stiffness and damping coefficients.

The kinematic requirement that a bearing be in equilibrium is that its velocity $\mathbf{V}$ relative to the stationary X, Y, Z system vanish, i.e., $C\dot{\epsilon} = C\epsilon\dot{\beta} = 0$. From equation (3), this yields the squeeze velocity $\mathbf{V}_{s0} = \mathbf{u}_\beta C\epsilon\bar{\omega} = \mathbf{K}\bar{\omega}\times C\boldsymbol{\epsilon}$ which physically means that the $\mathbf{u}_\epsilon$ squeeze velocity component is zero; hence from Fig. 9(a) $\alpha = \alpha_0 = \pi/2$ at equilibrium. For the impedance plots of Fig. 3, $\alpha = +\pi/2$ is the line $x = 0$; i.e., the y axis. This statement can be better appreciated by noting that $\mathbf{V}_s$ is parallel to the x axis, and it is only on the y axis that the eccentricity and squeeze-velocity vectors are perpendicular.

To define the direction of ϵ_0 (the equilibrium eccentricity ratio) and $\mathbf{V}_{s0}$ relative to the stationary X, Y, Z axes, we assume (without loss

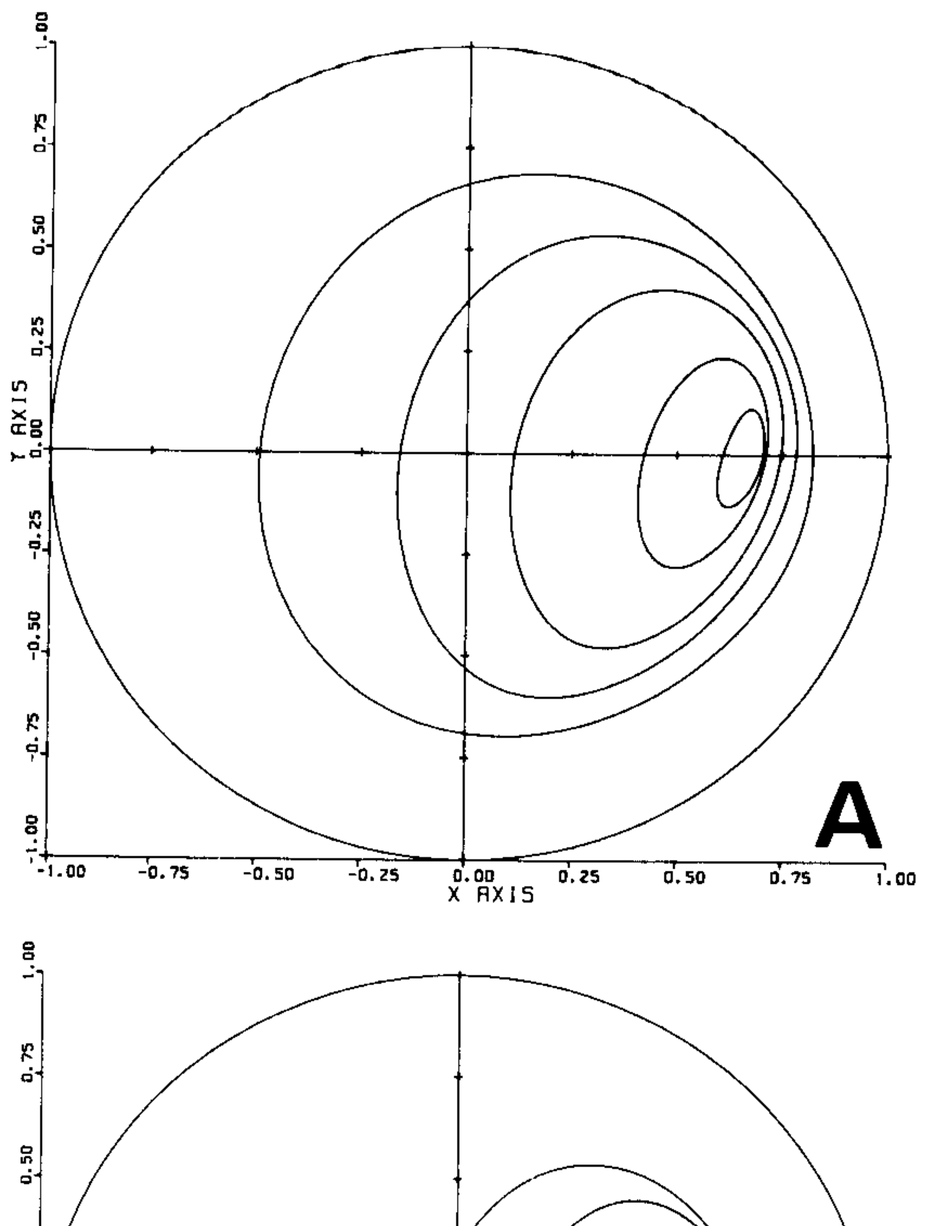

Fig. 7 Transient simulation results using the finite-length impedance model of equations (29)–(32) for comparison with Tonneson's experimental results (Fig. 5)

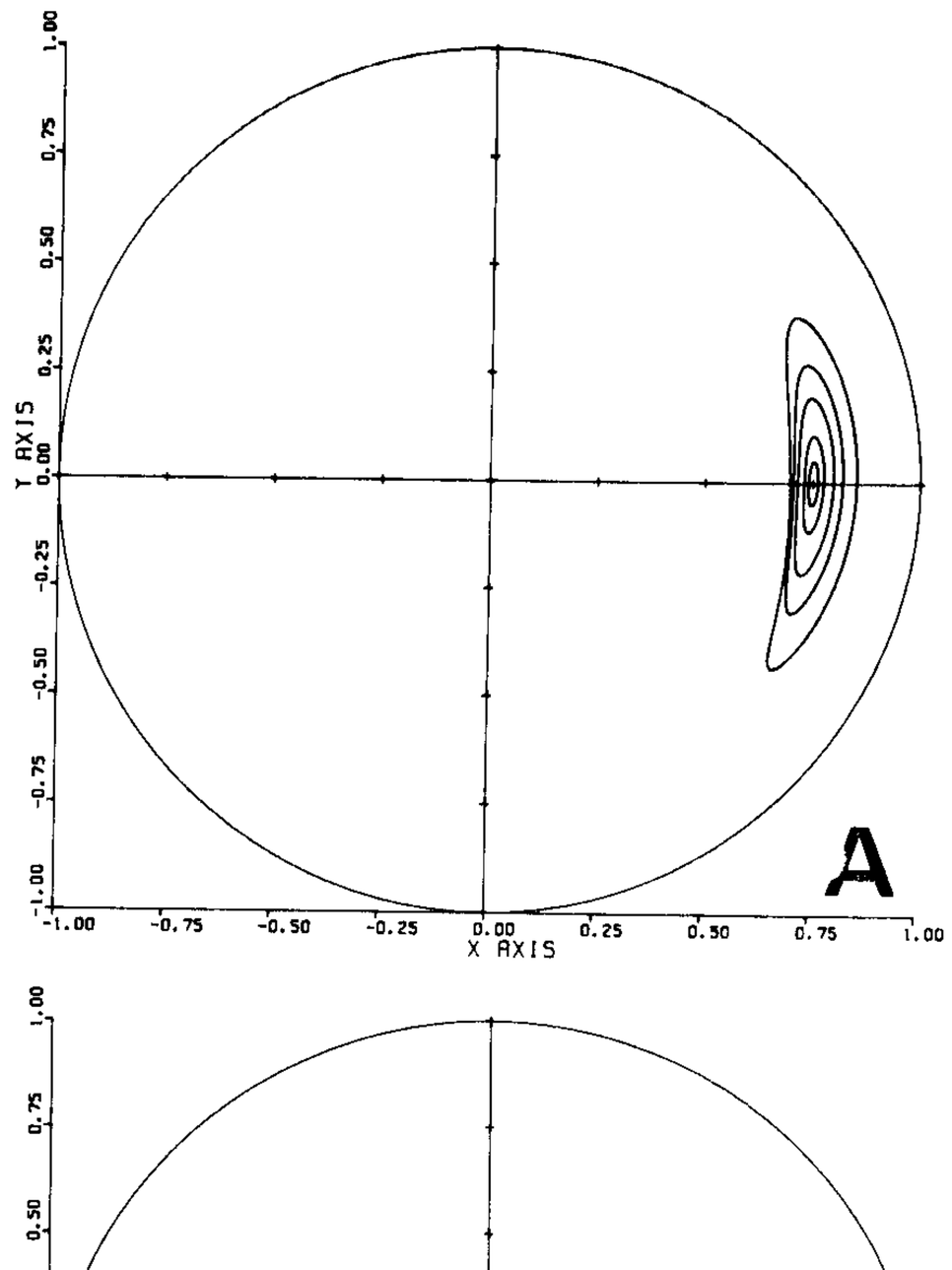

Fig. 8 Transient simulation results using the 2π Ocvirk impedance model for comparison with Tonneson's experimental results (Fig. 5)

of generality) that the applied static load is directed along the $-Y$ axis. Hence, the reaction load F_0 is directed along the $+Y$ axis, and from Figs. 2 and 9(a) we have at equilibrium $\beta_0 = -(\pi/2 - \gamma_0)$, where γ_0 is defined by the last of equation (26) as

$$tg\gamma_0 = -W_\beta(\epsilon_0, \pi/2)/W_\epsilon(\epsilon_0, \pi/2), \tag{40}$$

Equation (40) defines the equilibrium locus of the rotor. The (familiar) form of this locus is illustrated in Fig. 10 for the finite-length impedance of equation (29)–(32). The solution for ϵ_0 is inherently a nonlinear problem, whose solution is parameterized in terms of the Sommerfeld number definition

$$S = \epsilon_0 W_0/2 = F_0(C/R)^2/2\mu\bar{\omega}LD;\ \bar{\omega} > 0 \tag{41}$$
$$W_0 = W(\epsilon_0, \pi/2)$$

This result is obtained by substituting the static force and squeeze-velocity magnitudes into the impedance definition, equation (14). Fig. 11 illustrates the form of equation (41) for the finite-length impedance definition of equations (29)–(32). The results of Figs. 10 and 11 coincide with previous finite-length calculations [25], and provide a static verification of the finite-length impedance definition.

At equilibrium, the $\mathbf{u}_\epsilon$, $\mathbf{u}_\beta$ reference system has a fixed position relative to the stationary coordinate system. Hence stiffness and damping coefficients will be defined in terms of the $\mathbf{u}_\epsilon$, $\mathbf{u}_\beta$ reference, and the similarity transformation

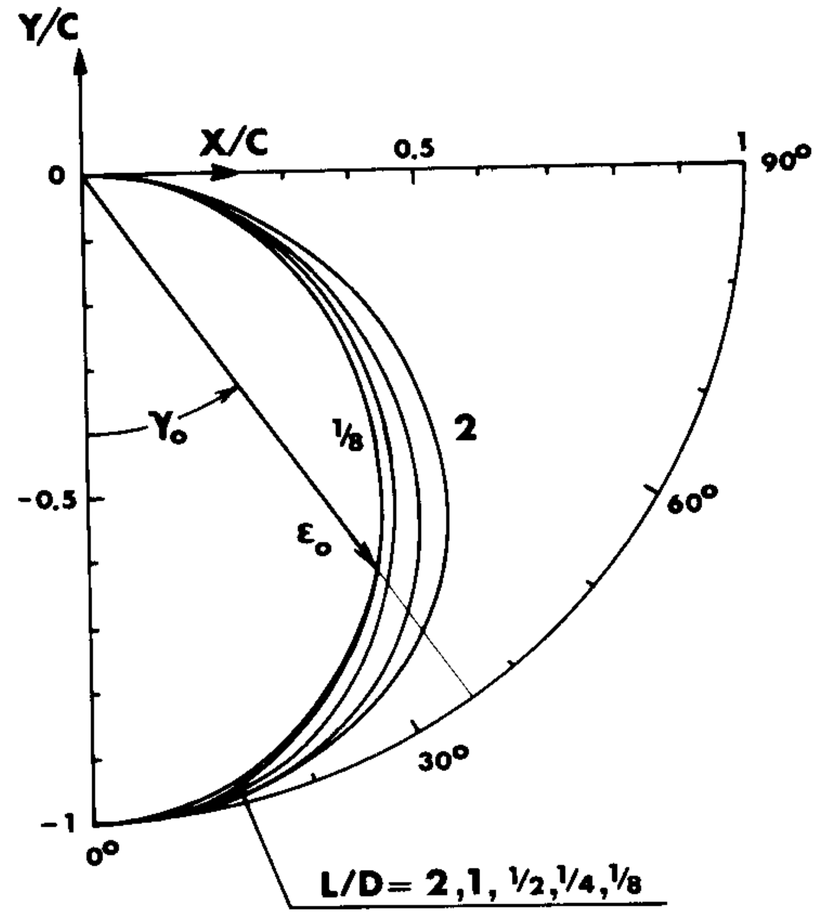

Fig. 10 Bearing equilibrium locus definition of equation (40) for the finite-length impedances of equations (29)–(32)

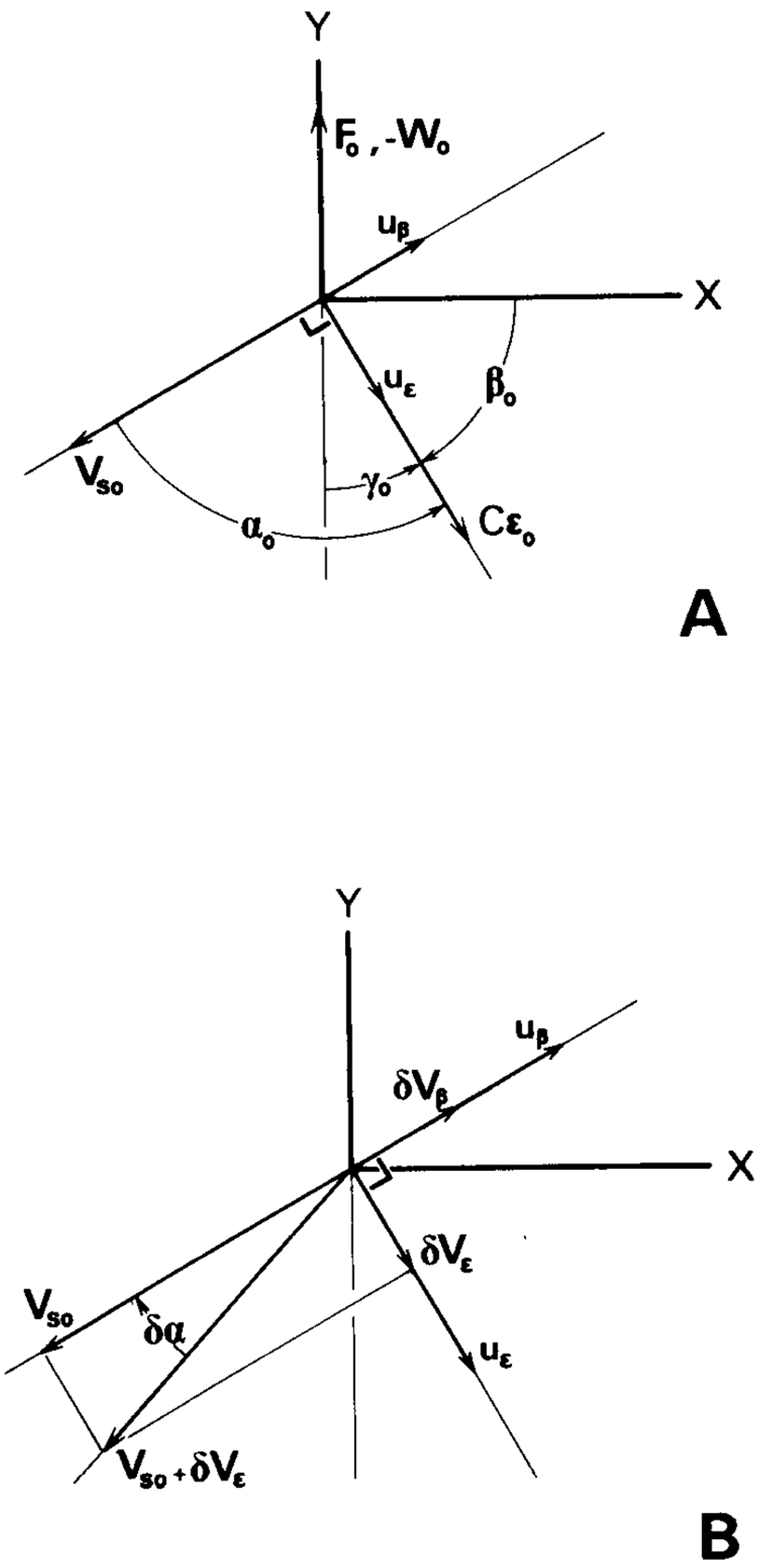

(*a*) static position,
(*b*) velocity perturbation

Fig. 9 Equilibrium conditions for plain journal bearings

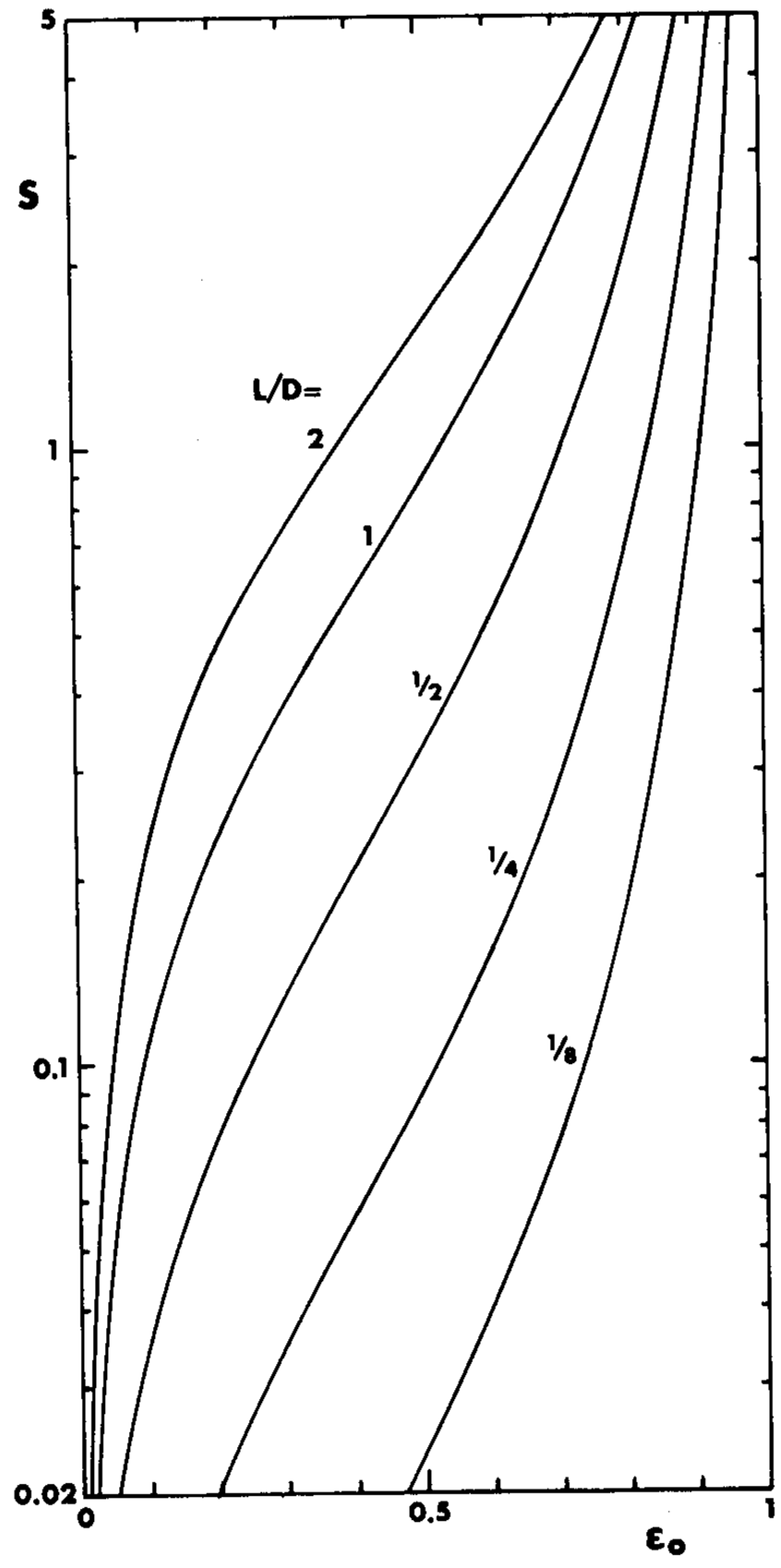

Fig. 11 Sommerfeld number solution, $S = \epsilon_0 W(\epsilon_0, \pi/2)/2$ from equation (41) for the finite-length impedances of equations (29)–(32)

$$[a_{I,J}] = [R_0]^T [a_{\epsilon,\beta}][R_0], \qquad [b_{I,J}] = [R_0]^T [b_{\epsilon,\beta}][R_0]$$

$$[R_0] = \begin{bmatrix} c\beta_0 s\beta_0 \\ -s\beta_0 c\beta_0 \end{bmatrix} = \begin{bmatrix} s\gamma_0 - c\gamma_0 \\ c\gamma_0 \quad s\gamma_0 \end{bmatrix} \tag{42}$$

will then be used to obtain their desired definition with respect to the X, Y axes.

A Taylor series expansion of the bearing reaction force about the equilibrium position yields

$$F_\epsilon(\epsilon, \beta, \dot{\epsilon}, \dot{\beta}) = F_\epsilon(\epsilon_0, \beta_0, 0, 0) + \frac{1}{C}\frac{\partial F_\epsilon}{\partial \epsilon} Cd\epsilon + \frac{1}{C\epsilon}\frac{\partial F_\epsilon}{\partial \beta} C\epsilon d\beta + \frac{1}{C}\frac{\partial F_\epsilon}{\partial \dot{\epsilon}} Cd\dot{\epsilon} + \frac{1}{C\epsilon}\frac{\partial F_\epsilon}{\partial \dot{\beta}} C\epsilon d\dot{\beta}$$

$$F_\beta(\epsilon, \beta, \dot{\epsilon}, \dot{\beta}) = F_\beta(\epsilon_0, \beta_0, 0, 0) + \frac{1}{C}\frac{\partial F_\beta}{\partial \epsilon} Cd\epsilon + \frac{1}{C\epsilon}\frac{\partial F_\beta}{\partial \beta} C\epsilon d\beta + \frac{1}{C}\frac{\partial F_\beta}{\partial \dot{\epsilon}} Cd\dot{\epsilon} + \frac{1}{C\epsilon}\frac{\partial F_\beta}{\partial \dot{\beta}} C\epsilon d\dot{\beta} \tag{43}$$

where second and higher order differential terms have been dropped. By definition, the components of $[a_{\epsilon,\beta}]$ and $[b_{\epsilon,\beta}]$ are seen to be

$$a_{\epsilon\epsilon} = -\frac{1}{C}\frac{\partial F_\epsilon}{\partial \epsilon} \qquad a_{\epsilon\beta} = -\frac{1}{C\epsilon}\frac{\partial F_\epsilon}{\partial \beta}$$

$$a_{\beta\epsilon} = -\frac{1}{C}\frac{\partial F_\beta}{\partial \epsilon} \qquad a_{\beta\beta} = -\frac{1}{C\epsilon}\frac{\partial F_\beta}{\partial \beta}$$

$$b_{\epsilon\epsilon} = -\frac{1}{C}\frac{\partial F_\epsilon}{\partial \dot{\epsilon}} \qquad b_{\epsilon\beta} = -\frac{1}{C\epsilon}\frac{\partial F_\epsilon}{\partial \dot{\beta}}$$

$$b_{\beta\epsilon} = -\frac{1}{C}\frac{\partial F_\beta}{\partial \dot{\epsilon}} \qquad b_{\beta\beta} = -\frac{1}{C\epsilon}\frac{\partial F_\beta}{\partial \dot{\beta}} \tag{44}$$

with the partial derivatives evaluated at the equilibrium position.

The coefficients $a_{\epsilon\epsilon}$, $a_{\beta\epsilon}$ may be obtained directly from the following restatement of equation (24)

$$\mathbf{F} = -2\mu L \left(\frac{R}{C}\right)^3 V_s \mathbf{W} \tag{45}$$

The partial derivative of this relationship with respect to ϵ yields

$$-\frac{1}{C}\frac{\partial \mathbf{F}}{\partial \epsilon} = 2\mu L \left(\frac{R}{C}\right)^3 \left\{\frac{1}{C}\frac{\partial V_s}{\partial \epsilon}\mathbf{W} + \frac{V_s}{C}\frac{\partial \mathbf{W}}{\partial \epsilon}\right\} \tag{46}$$

As noted previously, at equilibrium $V_s = V_{s0} = C\epsilon_0\bar{\omega}$; hence from equations (44), (45), and (46)

$$a_{\epsilon\epsilon} = \frac{F_0}{CW_0}\left(\frac{W_\epsilon}{\epsilon_0} + \frac{\partial W_\epsilon}{\partial \epsilon}\right)$$

$$a_{\beta\epsilon} = \frac{F_0}{CW_0}\left(\frac{W_\beta}{\epsilon_0} + \frac{\partial W_\beta}{\partial \epsilon}\right) \tag{47}$$

From equation (40), these relationships have the alternative form

$$a_{\epsilon\epsilon} = \frac{F_0}{C}\left(\frac{c\gamma_0}{\epsilon_0} - s\gamma_0\frac{\partial \gamma}{\partial \epsilon} + c\gamma_0\frac{\partial W}{\partial \epsilon}\right)$$

$$a_{\beta\epsilon} = -\frac{F_0}{C}\left(\frac{s\gamma_0}{\epsilon_0} + c\gamma_0\frac{\partial \gamma}{\partial \epsilon} + s\gamma_0\frac{\partial W}{\partial \epsilon}\right) \tag{48}$$

The coefficients $a_{\epsilon\beta}$, $a_{\beta\beta}$ are obtained by considering the consequences of a perturbation $\delta\beta_0$ of the equilibrium angle β_0, with ϵ_0, α_0, and the reaction force magnitude held constant. The rotation of $\delta\beta_0$ yields

$$F_\epsilon = F_{\epsilon 0}c(\delta\beta_0) + F_{\beta 0}s(\delta\beta_0) \cong F_{\epsilon 0} + F_{\beta 0}\delta\beta_0$$

$$F_\beta = -F_{\epsilon 0}s(\delta\beta_0) + F_{\beta 0}c(\delta\beta_0) \cong F_{\beta 0} - F_{\epsilon 0}\delta\beta_0$$

By comparison to equation (43), the desired coefficients are

$$a_{\epsilon\beta} = \frac{-F_{\beta 0}}{C\epsilon_0} = -\frac{F_0}{C\epsilon_0}\frac{W_{\beta 0}}{w_0} = \frac{F_0}{C}\frac{s\gamma_0}{\epsilon_0}$$

$$a_{\beta\beta} = \frac{F_{\epsilon 0}}{C\epsilon_0} = \frac{F_0}{C\epsilon_0}\frac{W_{\epsilon 0}}{w_0} = \frac{F_0}{C}\frac{c\gamma_0}{\epsilon_0} \tag{49}$$

Fig. 9(b) illustrates the two perturbed velocity components $\delta V_\epsilon = C\delta\dot{\epsilon}$, $\delta V_\beta = C\epsilon\delta\dot{\beta}$, and assists in the derivation of damping coefficients. The direct consequence of the change δV_ϵ (with $\delta V_\beta = 0$ and constant ϵ_0, β_0) is the perturbation $\delta\alpha$. From Fig. 9(b),

$$\frac{d\alpha}{dV_\epsilon} = \frac{-1}{V_{s0}}$$

Hence, from equation (45)

$$-\frac{\partial \mathbf{F}}{\partial V_\epsilon} = 2\mu L\left(\frac{R}{C}\right)^3 V_s \frac{\partial \mathbf{W}}{\partial \alpha}\frac{d\alpha}{dV} = \frac{-F}{WV_{s0}}\frac{\partial \mathbf{W}}{\partial \alpha}$$

By comparison to equations (43) and (44),

$$b_{\epsilon\epsilon} = \frac{-F_0}{W_0V_{s0}}\frac{\partial W_\epsilon}{\partial \alpha} = \frac{-F_0}{C\bar{\omega}\epsilon_0}\left(\frac{c\gamma_0}{W_0}\frac{\partial W}{\partial \alpha} - s\gamma_0\frac{\partial \gamma}{\partial \alpha}\right)$$

$$b_{\beta\epsilon} = \frac{-F_0}{W_0V_{s0}}\frac{\partial W_\beta}{\partial \alpha} = \frac{F_0}{C\bar{\omega}\epsilon_0}\left(\frac{s\gamma_0}{W_0}\frac{\partial W}{\partial \alpha} + c\gamma_0\frac{\partial \gamma}{\partial \alpha}\right) \tag{50}$$

The perturbed velocity component δV_β is seen from Fig. 9(b) to yield directly $\delta V_s = -\delta V_\beta$; hence $dV_s/dV_\beta = -1$, and from equation (45),

$$-\frac{\partial \mathbf{F}}{\partial V_\beta} = 2\mu L\left(\frac{R}{C}\right)^3 \mathbf{W}\frac{dV_s}{dV_\beta} = -2\mu L\left(\frac{R}{C}\right)^3 \mathbf{W}_0$$

By comparison to equations (43) and (44), the remaining damping coefficients are

$$b_{\epsilon\beta} = \frac{-F_0}{W_0V_{s0}}W_{\epsilon 0} = \frac{-F_0}{C\bar{\omega}}\left(\frac{c\gamma_0}{\epsilon_0}\right)$$

$$b_{\beta\beta} = \frac{-F_0}{W_0V_{s0}}W_{\beta 0} = \frac{F_0}{C\bar{\omega}}\left(\frac{s\gamma_0}{\epsilon_0}\right) \tag{51}$$

For convenience, the following normalized coefficient definitions are employed

$$\bar{a}_{ij} = (C/F_0)a_{ij}, \qquad \bar{b}_{ij} = (2C\bar{\omega}/F_0)b_{ij} \tag{52}$$

From this relationship and equation (42), the following complete set of dimensionless stiffness and damping coefficients is obtained.

$$\bar{a}_{XX} = \frac{c\gamma}{\epsilon} - s\gamma\left(\frac{\partial \gamma}{\partial \epsilon}\right)_\alpha$$

$$\bar{a}_{XY} = \frac{s\gamma}{\epsilon} + c\gamma\left(\frac{\partial \gamma}{\partial \epsilon}\right)_\alpha$$

$$\bar{a}_{YX} = \frac{-s\gamma}{\epsilon} - \frac{s\gamma}{W}\left(\frac{\partial W}{\partial \epsilon}\right)_\alpha$$

$$\bar{a}_{YY} = \frac{c\gamma}{\epsilon} + \frac{c\gamma}{W}\left(\frac{\partial W}{\partial \epsilon}\right)_\alpha$$

$$\bar{b}_{XX} = \frac{2s\gamma}{\epsilon}\left(\frac{\partial \gamma}{\partial \alpha}\right)_\epsilon$$

$$\bar{b}_{XY} = \frac{-2c\gamma}{\epsilon}\left(\frac{\partial \gamma}{\partial \alpha}\right)_\epsilon$$

$$\bar{b}_{YX} = \frac{2}{\epsilon}\left\{c\gamma + \frac{s\gamma}{\mathrm{W}}\left(\frac{\partial W}{\partial \alpha}\right)_\epsilon\right\}$$

$$\bar{b}_{YY} = \frac{2}{\epsilon}\left\{s\gamma - \frac{c\gamma}{W}\left(\frac{\partial W}{\partial \alpha}\right)_\epsilon\right\} \tag{53}$$

Note that these coefficients are to be evaluated at an equilibrium position, and that they apply for any impedance definition, e.g., short, long, finite-length etc. The spring and damping coefficients which result from applying these relationships to the finite-length impedance of equations (29)–(32) are stated in Appendix B, and illustrated in Fig. 12. The results basically coincide with those of references [17] and [18] except at large and small eccentricities, where the numerical differentiation approach presumably encounters difficulties.

The derivation of stiffness and damping coefficients for bearings is based on the assumption of small motion about an equilibrium position. This assumption is not valid for squeeze-film dampers, since a damper is not designed to react a static load, and has a minimal in-

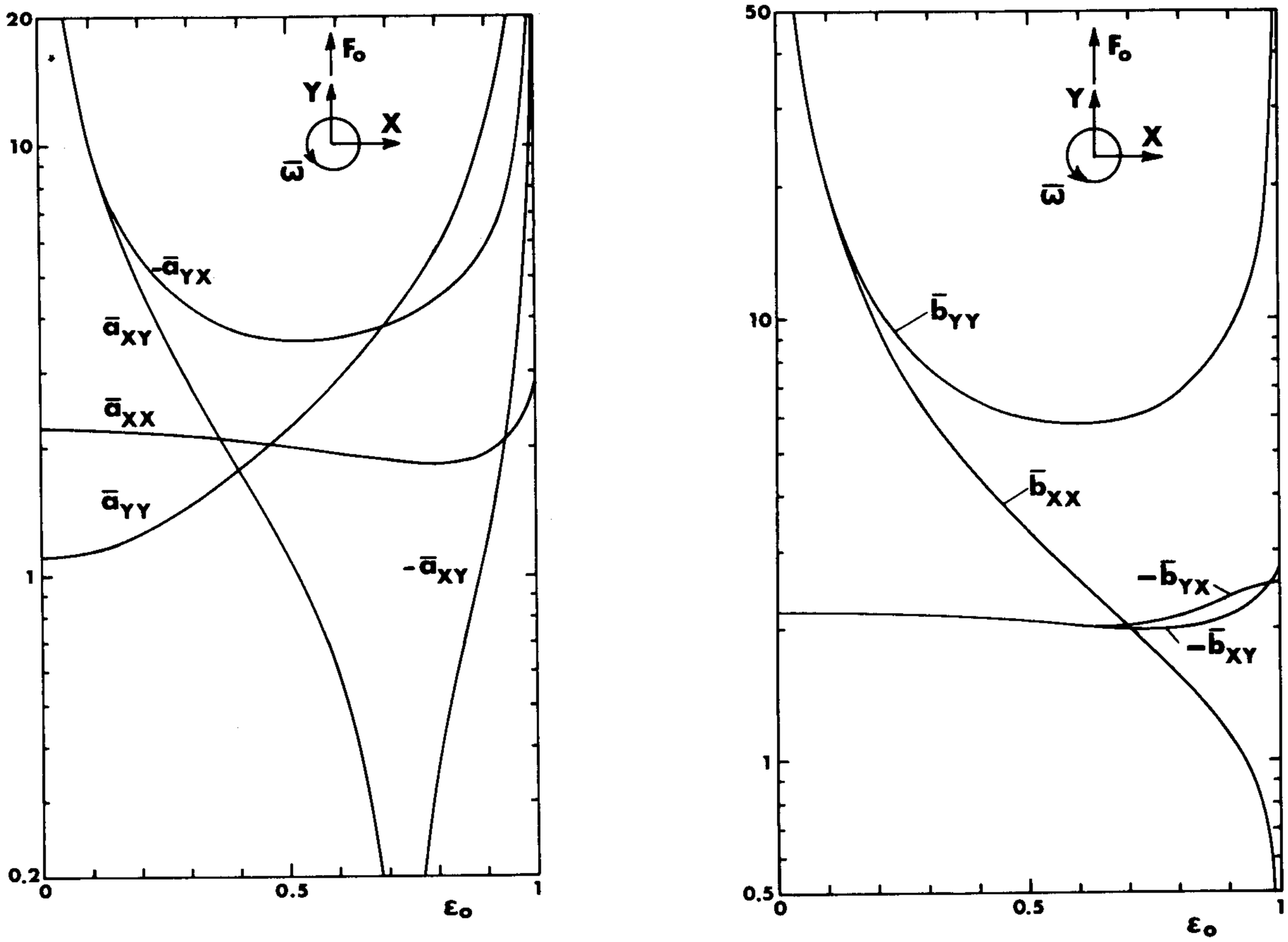

Fig. 12 (*a*) **Stiffness and** (*b*) **damping coefficients for the finite-length impedances of equations (29)–(32) with** $L/D = 1$

fluence on a rotor's static equilibrium position. Tonneson [9] employs the model

$$F_X = -B_X\dot{X}, \qquad F_Y = -B_Y\dot{Y} \tag{54}$$

for small motion of the form

$$X = C\epsilon_0 + \Delta c(\Omega t), \qquad Y = \Delta s(\Omega t)$$

The coefficients B_X, B_Y are obtained by considering (separately) velocity perturbations in the X and Y directions, and then calculating the average damping coefficient over the period $T = 2\pi/\Omega$. Tonneson's experimental results demonstrate that the comparatively crude model of equation (54) is valid for short dampers at small eccentricity ratios. The damping coefficients of equation (54) can be defined for a noncavitating 2π bearing by

$$B_X(2\pi) = 2\mu L(R/C)^3 W_\epsilon(\epsilon_0, 0),$$

$$B_Y(2\pi) = 2\mu L\left(\frac{R}{C}\right)^3 W_\beta\left(\epsilon_0, -\frac{\pi}{2}\right) \tag{55}$$

where W_ϵ, W_β are components of the appropriate 2π impedance. The corresponding coefficients for a cavitating bearing are simply $B_X(\pi) = B_X(2\pi)/2$, $B_Y(\pi) = B_Y(2\pi)/2$.

Coefficient definitions for finite-length dampers (which are comparable to the short-bearing coefficients developed by Tonneson) are obtained from solution 5 of Appendix A. Note that the model of equation (54) is only valid at small eccentricity ratios, and a nonlinear transient analysis is appropriate at other operating conditions.

Rotor Stability Analysis

The linear stability of a symmetrical rigid rotor on plain journal bearings is readily determined via the stiffness and damping coefficients of the preceding section. The appropriate dimensionless differential equations for (small) motion about an equilibrium position are

$$\frac{mC}{F_0}\dot{\phi}^2\begin{Bmatrix} X'' \\ Y'' \end{Bmatrix} + [\bar{b}_{I,J}]\begin{Bmatrix} X' \\ Y' \end{Bmatrix} + [\bar{a}_{I,J}]\begin{Bmatrix} X \\ Y \end{Bmatrix} = 0 \tag{56}$$

where the "′" denotes differentiation with respect to the dimensionless time variable $\tau = \dot{\phi}t$. This equation is obtained from equations (34), (39) and (52). The results of a Routh-Hurwitz stability analysis of equation (56) for the stiffness and damping coefficients of Appendix B are given in Fig. 13 for a range of "dimensionless bearing loads" defined as

$$\frac{C^4}{R^4}\cdot\frac{mC}{\mu^2 D^4}F_0$$

This figure illustrates the dimensionless onset speed of instability

$$\frac{C^2}{R^2}\cdot\frac{mC}{\mu D^2}\dot{\phi}_c$$

as a function of the dimensionless load, and the L/D and eccentricity ratios. These results emphasize the (sharply) destabilizing effect of an increase in bearing length.

Summary and Concluding Comments

The bearing impedance vector has been introduced, and defines the bearing reaction force components as a function of the bearing motion. Impedances are derived directly for the Ocvirk (short) and Sommerfeld (long) bearings, and the relationships between the impedance vector **W** and the more familiar mobility vector **M** are developed and used to derive analytic impedances for finite-length bearings. The static correctness of the cavitating finite-length impedance is verified by the presentation of both equilibrium loci plots and plots of Sommerfeld number versus (equilibrium) eccentricity ratio for a range of (L/D) ratios. Analytic stiffness and damping coefficient

definitions are derived in terms of an impedance vector for small motion about an equilibrium position, and demonstrated for the finite-length cavitating impedance. These coefficients are used for stability analysis of a symmetrically supported rotor, with results presented as a function of the L/D ratio. Damping coefficients are also stated for finite-length squeeze-film dampers comparable to those of Tonneson [9].

Nonlinear transient rotordynamic simulations are presented for the short π and 2π impedances and the finite-length cavitating impedance. The finite-length impedance yields more accurate results for substantially less computer time than the short-bearing, numerical-pressure-integration approach of references [5]–[8].

The results of this study demonstrate that the impedance vector and its associated stiffness and damping coefficients are an attractive and comprehensive approach for modeling plain journal bearings (and squeeze-film dampers) in rotordynamics work. Further, the finite-length cavitating (equations (29)–(32)) and 2π (Solution 5, Appendix A) impedances developed here are markedly superior to presently employed analytic bearing models, i.e., the Ocvirk, Sommerfeld, or Warner Sommerfeld models. These impedances provide very accurate models for all (L/D) and eccentricity ratios of general interest.

The following direct extensions of the present work are judged to be feasible:

(a) Nonlinear impedances and stiffness and damping coefficients can be calculated for pivoted pad bearings, subject to the restriction that the pad's rotational dynamics be negligible. Ten Napel, Moes, and Bosma [26] have demonstrated the feasibility of a mobility description for this type of bearing.

(b) Simandiri and Hahn [8] have used the short-bearing model with a finite supply pressure to examine the effect of supply pressure on the behavior of squeeze-film dampers. The effect of both supply and discharge pressure can be accounted for in the numeric calculation of a finite-length bearing impedance, and calculation of stiffness and damping coefficients from such an impedance follows from equation (53).

The following extensions of the present work appear to be feasible, but are less immediate:

(a) Narrow-grooved plain journal bearings appear to be amenable to mobility-impedance approaches by a restatement of the Reynolds equation.

(b) Lobed bearings for which all lobes are at high eccentricity ratios also seem to be subject to a mobility-impedance analysis procedure.

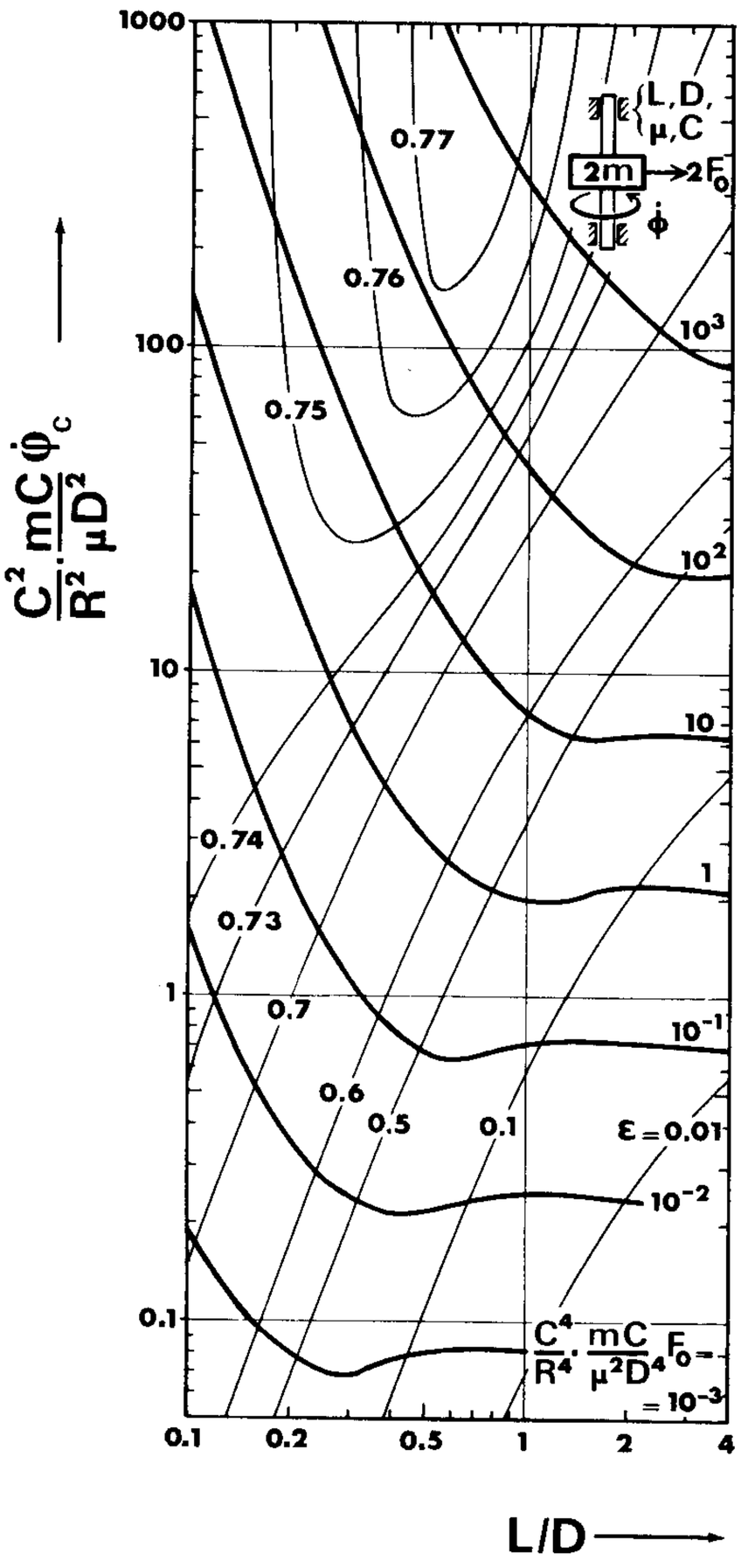

Fig. 13 Dimensionless onset speed of instability for a rotor on plain journal bearings versus the *L/D* ratio for a range of bearing numbers

References

1 Booker, J. F., "Dynamically Loaded Journal Bearings: Mobility Method of Solution," *Journal of Basic Engineering*, TRANS. ASME, Sept. 1965, pp. 537–546.

2 Booker, J. F., "Dynamically Loaded Journal Bearings: Maximum Film Pressure," JOURNAL OF LUBRICATION TECHNOLOGY, TRANS. ASME, July 1969, pp. 534–543.

3 Booker, J. F., "Dynamically Loaded Journal Bearings: Numerical Application of the Mobility Method," JOURNAL OF LUBRICATION TECHNOLOGY, TRANS. ASME, Jan. 1971, pp. 168–176, and Apr. 1971, p. 315.

4 Blok, H., "Topological Aspects and the Impulse/Whirl Angle Method in the Orbital Hydrodynamics of Dynamically Loaded Journal Bearings," Lecture notes (condensed English version), Delft, The Netherlands, Aug. 1965.

5 Kirk, R. G., and Gunter, E. J., "Transient Journal Bearing Analysis," NASA CR 1599, June 1970.

6 Kirk, R. G., and Gunter, E. J., "Short Bearing Analysis Applied to Rotor Dynamics, Part 1: Theory," Paper No. 75-Lub-30, ASLE-ASME Joint Lubrication Conference, Oct. 1975.

7 Kirk, R. G., and Gunter, E. J., "Short Bearing Analysis Applied to Rotor Dynamics, Part 2: Results of Journal Bearing Response," Paper No. 75-Lub-31, ASLE-ASME Joint Lubrication Conference, Oct. 1975.

8 Simandiri, S., and Hahn, E. J., "Effect of Pressurization in the Vibration Isolation Capability of Squeeze Film Bearings," ASME Paper No. 75-DET-70, Design Engineering Technology Conference, Washington, D. C., 1975.

9 Tonneson, J., "Experimental Parametric Study of a Squeeze Film Bearing," Paper No. 75-Lub-42, ASLE-ASME Joint Lubrication Conference, Miami Beach, Fla., 1975.

10 Vance, J. M., and Kirton, A. J., "Experimental Measurement of the Dynamic Force Response of a Squeeze-Film Bearing Damper," ASME Paper No. 75-DET-39, *Design Engineering Technology Conference*, Washington, D. C., 1975.

11 Warner, P. C., "Static and Dynamic Properties of Partial Journal Bearings," *Journal of Basic Engineering*, TRANS. ASME, Series D, Vol. 85, 1963, p. 247–257.

12 Myrick, S. T., Jr., and Rylander, H. G., "Analysis of Flexible Rotor Whirl and Whip Using a Realistic Hydrodynamic Journal Bearing Model," ASME Paper No. 75-DET-68, Design Engineering Technology Conference, Washington, D. C., 1975.

13 Moes, H., and Herrebrugh, K., "An Approximation Formula for the Mobility Function of Full Cylindrical Journal Bearings of Finite Length," Appendix VII by lecture notes reference [4] of Prof. H. Blok, 1965.

14 Moes, H., Discussion, I. Mech. E., 1969 Tribology Convention, Gothenburg, *Proceedings of the Institute of Mechanical Engineers*, Vol. 183, Part 3P, 1968–1969, pp. 205–206. Because of a printing error the expression for M_y in this discussion has to be multiplied by y.

15 Campbell, J., Love, P. P., Martin, F. A., and Rafique, S. O., "Bearings for Rotating Machinery: A Review of the Present State of Theoretical, Experimental, and Service Knowledge," *Proceedings Institute Mechanical Engineers*, Vol. 182, Pt. 3A, pp. 51–74.

16 Lund, J. W., and Sternlicht, B., "Rotor Bearing Dynamics with Emphasis on Attenuation," *Journal of Basic Engineering*, TRANS. ASME, Dec. 1962, pp. 491–502.

17 Orcutt, F. K., and Arwas, E. B., "The Steady-State and Dynamic Characteristics of a Full Circular Bearing and a Partial Arc Bearing in the Laminar and Turbulent Flow Regimes," *Journal of Lubrication Technology*, TRANS. ASME, Vol. 89, Series F, No. 2, Apr. 1967, pp. 143–153.

18 Reinhoudt, J. P., "On the Stability of Rotor-And-Bearing Systems and on the Calculation of Sliding Bearings," PhD thesis, Technical University of Eindhoven (The Netherlands), 1972.

19 Lund, J. W., "Calculation of Stiffness and Damping Properties of Gas Bearings," JOURNAL OF LUBRICATION TECHNOLOGY, TRANS. ASME, Oct. 1968, pp. 793–803.

20 Moes, H., "Hydrodynamic Lubrication, capita selecta." (In Dutch).

Abstract of series of lectures to students of Twente University of Technology, Spring 1974 (revised: Summer 1975), pp. 24–32.

21 Gross, H. A., *Gas Film Lubrication,* Wiley, New York, N. Y., 1962.

22 Childs, Dara W., "Two Jeffcott-Based Modal Simultation Models for Flexible Rotating Equipment," *Journal of Engineering for Industry*, TRANS. ASME, Aug. 1975, pp. 1000–1014.

23 Childs, Dara W., "A Modal Transient Simulation Model for Flexible Asymmetric Rotors," Paper No. 75-DET-34, ASME Design Engineering Technical Conference, Washington, D. C., Sept. 17–19, 1975, to be published in *Journal of Engineering for Industry.*

24 Childs, Dara W., "A Modal Transient Rotordynamic Model for Dual-Rotor Jet Engine Systems," ASME Paper No. 75-DE-S, to be published in *Journal of Engineering for Industry,* TRANS. ASME.

25 Pinkus, O. and Sternlicht, B., *Theory of Hydrodynamic Lubrication,* McGraw-Hill, New York, N. Y., 1961.

26 Ten Napel, W. E., Moes, H., and Bosma, R., "Dynamically Loaded Pivoted Pad Journal Bearings: Mobility Method of Solution," ASME Paper No. 75-Lub-25, ASLE-ASME Joint Lubrication Conference, Miami Beach, Fla., Oct. 1975.

27 Booker, J. F., "A Table of the Journal-Bearing Integral," *Journal of Basic Engineering*, TRANS. ASME, June 1965, pp. 533–535.

APPENDIX A

Impedance Definitions

1 2π-Ocvirk solution

$$W_\epsilon = 2\pi(1+2\epsilon^2)(1-\epsilon^2)^{-5/2}(L/D)^2 c\alpha$$

$$W_\beta = -2\pi(1-\epsilon^2)^{-3/2}(L/D)^2 s\alpha$$

2 π-Ocvirk solution for $\epsilon \simeq 0$

$$W = \pi(1-\xi)^{-5/2}(L/D)^2\left\{1+\frac{16}{\pi^2}\eta^2(1-\xi)^{-2}\right\}^{-1/2}$$

$$tg(\gamma-\alpha) = \frac{4}{\pi}\epsilon s\gamma/(1-\epsilon c\gamma)$$

or

$$\gamma \cong \{1-\xi'(1-\eta'^2)^{-1/2}\}\left[tg^{-1}\lambda - \frac{\pi}{2}\eta'/|\eta'| + s^{-1}(\eta')\right] + \alpha - s^{-1}(\eta')$$

with

$$\xi = \epsilon c\gamma \qquad \eta = \epsilon s\gamma \qquad \lambda = 2^{1/2}\{\lambda' - 2(4-\pi)\eta'^2/\pi - 1\}^{1/2}(\lambda'-1)^{-1/2}$$

$$\xi' = \epsilon c\alpha \qquad \eta' = \epsilon s\alpha \qquad \lambda' = \{1+16\pi^{-2}(4-\pi)\eta'^2\}$$

3 2π-Warner Sommerfeld solution (for Π see Booker [1])

$$W_\epsilon = 6\pi(1-\epsilon^2)^{-3/2}c\alpha\Pi$$

$$W_\beta = -12\pi\ (1-\epsilon^2)^{-1/2}(2+\epsilon^2)^{-1}s\alpha\Pi$$

4 π-Warner Sommerfeld solution

$$W = 3\pi 2^{-1/2}(1-\xi)^{-3/2}\left\{1+\frac{9}{16}\eta^2(1-\xi)^{-2}\right\}^{-1/2}\Pi$$

$$tg(\gamma-\alpha) = \frac{3}{4}\epsilon s\gamma/(1-\epsilon c\gamma)$$

or

$$\gamma \cong \{1-\xi'(1-\eta'^2)^{-1/2}\}\left[tg^{-1}\lambda - \frac{\pi}{2}\eta'/|\eta'| + s^{-1}(\eta')\right] + \alpha - s^{-1}(\eta')$$

$$\lambda = 2\{\eta'^2 - 2 + (4-3\eta'^2)^{1/2}\}^{1/2}/\{2-(4-3\eta'^2)^{1/2}\}$$

5 2π-Finite bearing solution

$$W_\epsilon = 6\pi(1-\epsilon^2)^{-3/2}c\alpha\{1+3(1-\epsilon^2)/(2+\epsilon^2)\cdot(L/D)^{-2}\}^{-1}$$

$$W_\beta = -12\pi(1-\epsilon^2)^{-1/2}(2+\epsilon^2)^{-1}s\alpha\{1 + 6(1-\epsilon^2)/(2+\epsilon^2)\cdot(L/D)^{-2}\}^{-1}$$

APPENDIX B

Formula for the Stiffness and Damping Constants for the Cavitating Finite Bearing Solution of equations (29)–(32).

The partial derivatives required to evaluate the stiffness and damping coefficients of equation (53) follow. The subscript 0 denotes evaluation at the equilibrium position.

$$a = 1 + 2.12B.$$

$$b = 1 + 3.60B.$$

$$\gamma_0 = tg^{-1}\{4a(1-\epsilon_0{}^2)^{1/2}/3b\epsilon_0\}$$

$$\xi_0 = \epsilon_0 c\gamma_0; \qquad \eta_0 = \epsilon_0 s\gamma_0$$

$$d = 1 - \xi_0$$

$$W_0 = \{0.150(E_0{}^2 + G_0{}^2)^{1/2}d^{3/2}\}^{-1}$$

$$\left(\frac{\partial\gamma}{\partial\epsilon}\right)_\alpha = \frac{4}{3}\{2(b-a)b^{-2} - a\epsilon_0{}^{-2}/b\}\, c^2\gamma_0(1-\epsilon_0{}^2)^{-1/2}$$

$$\left(\frac{\partial\gamma}{\partial\alpha}\right)_\epsilon = 1 + \left\{\gamma_0 - \frac{\pi}{2} + s^{-1}(\epsilon_0)\right\}\epsilon_0(1-\epsilon_0{}^2)^{-1/2}$$

$$\left(\frac{\partial W}{\partial\xi}\right)_\eta = -W_0\left[(E_0{}^2+G_0{}^2)^{-1}\left\{\frac{3}{4}G_0\eta_0 d^{-2} - 2.12E_0(L/D)^{-2}\right\} - \frac{3}{2}d\right]$$

$$\left(\frac{\partial W}{\partial\eta}\right)_\xi = -W_0(E_0{}^2+G_0{}^2)^{-1}G_0{}^2/\eta_0$$

$$\left(\frac{\partial\xi}{\partial\epsilon}\right)_\alpha = \left(\frac{\partial\xi}{\partial\epsilon}\right)_\gamma + \left(\frac{\partial\xi}{\partial\gamma}\right)_\epsilon\cdot\left(\frac{\partial\gamma}{\partial\epsilon}\right)_\alpha = c\gamma_0 - \epsilon_0 s\gamma_0\left(\frac{\partial\gamma}{\partial\epsilon}\right)_\alpha$$

$$\left(\frac{\partial\eta}{\partial\epsilon}\right)_\alpha = \left(\frac{\partial\eta}{\partial\epsilon}\right)_\gamma + \left(\frac{\partial\eta}{\partial\gamma}\right)_\epsilon\cdot\left(\frac{\partial\gamma}{\partial\epsilon}\right)_\alpha = s\gamma_0 + \epsilon_0 c\gamma_0\left(\frac{\partial\gamma}{\partial\epsilon}\right)_\alpha$$

$$\left(\frac{\partial\xi}{\partial\gamma}\right)_\epsilon = -\epsilon_0 s\gamma_0$$

$$\left(\frac{\partial\eta}{\partial\gamma}\right)_\epsilon = \epsilon_0 c\gamma_0$$

$$\left(\frac{\partial W}{\partial\epsilon}\right)_\alpha = \left(\frac{\partial W}{\partial\xi}\right)_\eta\cdot\left(\frac{\partial\xi}{\partial\epsilon}\right)_\alpha + \left(\frac{\partial W}{\partial\eta}\right)_\xi\cdot\left(\frac{\partial\eta}{\partial\epsilon}\right)_\alpha$$

$$\left(\frac{\partial W}{\partial\gamma}\right)_\epsilon = \left(\frac{\partial W}{\partial\xi}\right)_\eta\cdot\left(\frac{\partial\xi}{\partial\gamma}\right)_\epsilon + \left(\frac{\partial W}{\partial\eta}\right)_\xi\cdot\left(\frac{\partial\eta}{\partial\gamma}\right)_\epsilon$$

$$\left(\frac{\partial W}{\partial\alpha}\right)_\epsilon = \left(\frac{\partial W}{\partial\gamma}\right)_\epsilon\cdot\left(\frac{\partial\gamma}{\partial\alpha}\right)_\epsilon$$

J. F. Booker[6]

What follows is a rather long commentary on concepts and a very short query on possible applications.

Successful computation methods are always compromises between accuracy, generality, speed, and cost. Factors of formal elegance and intuitive appeal probably also play peripheral roles. The mobility method has proved to be a useful compromise; one hopes that the closely-related impedance method may find its niche as well.

The impedance and mobility methods form a perfect dual. Both provide for the efficient storage of bearing characteristics based on *any* suitable film model. Because pressure distributions are *not* calculated, both methods permit extremely efficient computation.

Though the methods are in one sense *inverse,* they should also be seen as *complementary* in view of their natural ranges of application: In the impedance method, instantaneous specification of eccentricity and velocity allows direct determination of force; in the mobility method, instantaneous specification of eccentricity and force allows direct determination of velocity. In appropriate applications the resulting equations of motion are in explicit form, and iterative calculations can be avoided entirely by the user in system simulation studies.

It seems productive to supplement the authors' detailed development with a concise user-oriented rationale of the two methods, proceeding from the special to the general by stages.

Special Case: Without Rotation

Impedance and mobility concepts are best understood in terms of experiments, analytical or physical, with nonrotating bearings. Such experiments attempt to relate instantaneously the journal center eccentricity (displacement) $\mathbf{e}$, squeeze velocity $\mathbf{V_s}$, and load force $\mathbf{F_L}$ or their dimensionless counterparts, eccentricity ratio ϵ, mobility $\mathbf{M}$, and impedance $\mathbf{W}$, defined by[7]

$$\epsilon = \frac{\mathbf{e}}{C}$$

$$\mathbf{M} = \frac{2\mu L}{(C/R)^3}\frac{\mathbf{V}_s}{|\mathbf{F}_L|}$$

$$\mathbf{W} = \frac{(C/R)^3}{2\mu L}\frac{\mathbf{F}_L}{|\mathbf{V}_s|}$$

so that

$$|\mathbf{W}||\mathbf{M}| = 1$$

The definitions of $\mathbf{M}$ and $\mathbf{W}$ clearly hinge on the proportionality of $|\mathbf{V_s}|$ and $|\mathbf{F_L}|$. This necessary proportionality is the *analytical* consequence of a linear Reynolds field equation with homogeneous boundary conditions and/or constraints. Alternatively, the proportionality is the *physical* consequence of an incompressible lubricant, both entering and cavitating (if at all) at near-ambient pressure.

The relation between eccentricity, velocity, and force can be displayed in "fixed" coordinates X,Y or in "moving" coordinates x,y and x',y' referenced, respectively, to velocity and force directions as shown in Fig. 14.

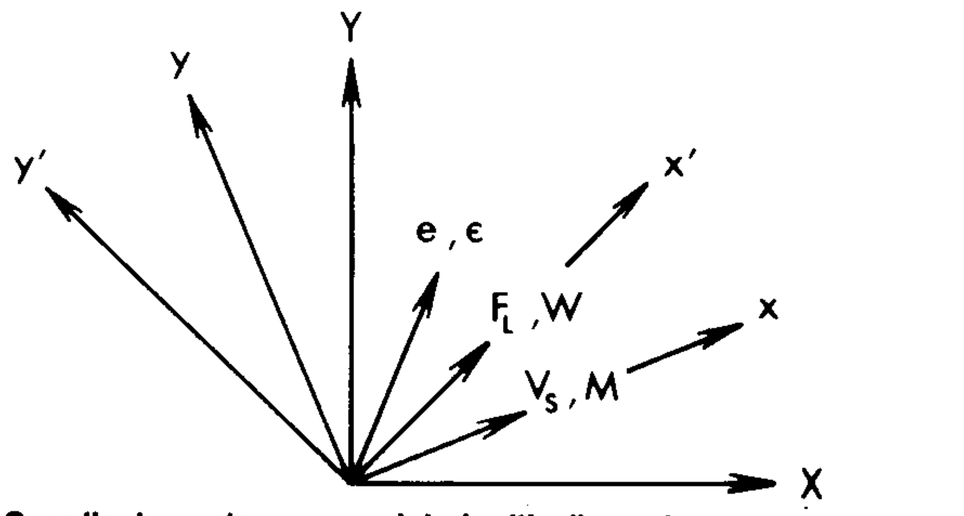

Fig. 14 Coordinate systems associated with dimensional/dimensionless eccentricity, velocity, and force vectors

Using the two "moving" frames, the same data can be displayed in alternate maps of impedance *or* mobility plotted over the clearance space of all possible eccentricity ratios. Figs. 15 and 16, kindly supplied by the authors, allow a comparison of typical impedance and mobility maps for the same basic data.[9] The two maps are oriented to velocity and force directions respectively as shown. Separate curvilinear families[11] indicate magnitude and direction of impedance and mobility vectors. Though specific to a particular length/diameter ratio,[10] such maps apply to all orientations of bearings with circumferential symmetry.

Either map, impedance or mobility, represents the complete relationship of eccentricity, velocity, and force for a particular bearing. Since the same basic data are displayed in both maps, each point on one map corresponds to a (different) point on the other,[12] and possession of one (entire) map permits construction of the other. This inverse relationship is immediately apparent along the midlines of the maps; elsewhere the connection is less obvious. The interested reader can verify that corresponding sample points are indicated in Figs. 15 and 16. As a further exercise he can examine the corresponding forms of the "equilibrium locus" whereon eccentricity and mobility (or velocity) vectors are perpendicular.

Availability of the *appropriate* map data is thus tantamount to solution of *all* problems involving the relation of eccentricity, velocity, and force for a particular non-rotating bearing. That is, specification of $\mathbf{e}$ and $\mathbf{V_s}$ allows direct determination of $\mathbf{F_L}$ via $\mathbf{W}$; alternatively, specification of $\mathbf{e}$ and $\mathbf{F_L}$ allows direct determination of $\mathbf{V_s}$ via $\mathbf{M}$. The *numerical* implementation of these procedures[13] can be described as follows:

---

[6] Associate Professor, School of Mechanical & Aerospace Engineering, Cornell University, Ithaca, N.Y.

[7] In the notation adopted by the authors, $\mathbf{W}$ is quite *literally* the inverse of $\mathbf{M}$. However, it should be noted that $\mathbf{W}$ is *not* the inverse mobility vector $\mathbf{M}^{-1}$ introduced in the writer's discussion of the closely-related impulse method of Blok [28].[8]

[8] See Additional References below.

[9] Actually, *two* sets of basic data are illustrated in each of Figs. 15 and 16. The left half of each map is based on the Ocvirk short bearing 2π (complete) film model; the right is based on the corresponding π (cavitated) film model. Thus each map may be expected to show increasing left-right symmetry in approaching the bottom center point.

[10] For the Ocvirk short bearing film model illustrated in Figs. 15 and 16 the dependence on length/diameter ratio is strong but simple: magnitudes of impedance (or mobility) vary directly (or inversely) with its square.

[11] The direction and magnitude families are generally *not* orthogonal, except along the midlines of both maps and portions of the impedance map boundary.

[12] Exceptionally, a point of vanishing mobility corresponds to a semicircle of infinite impedance.

[13] Essentially the same numerical procedures can be used to transform *non*dimensional quantities as well. i.e., specification of ϵ and $\mathbf{M}$ allows determination of $\mathbf{W}$; alternatively, specification of ϵ and $\mathbf{W}$ allows determination of $\mathbf{M}$.

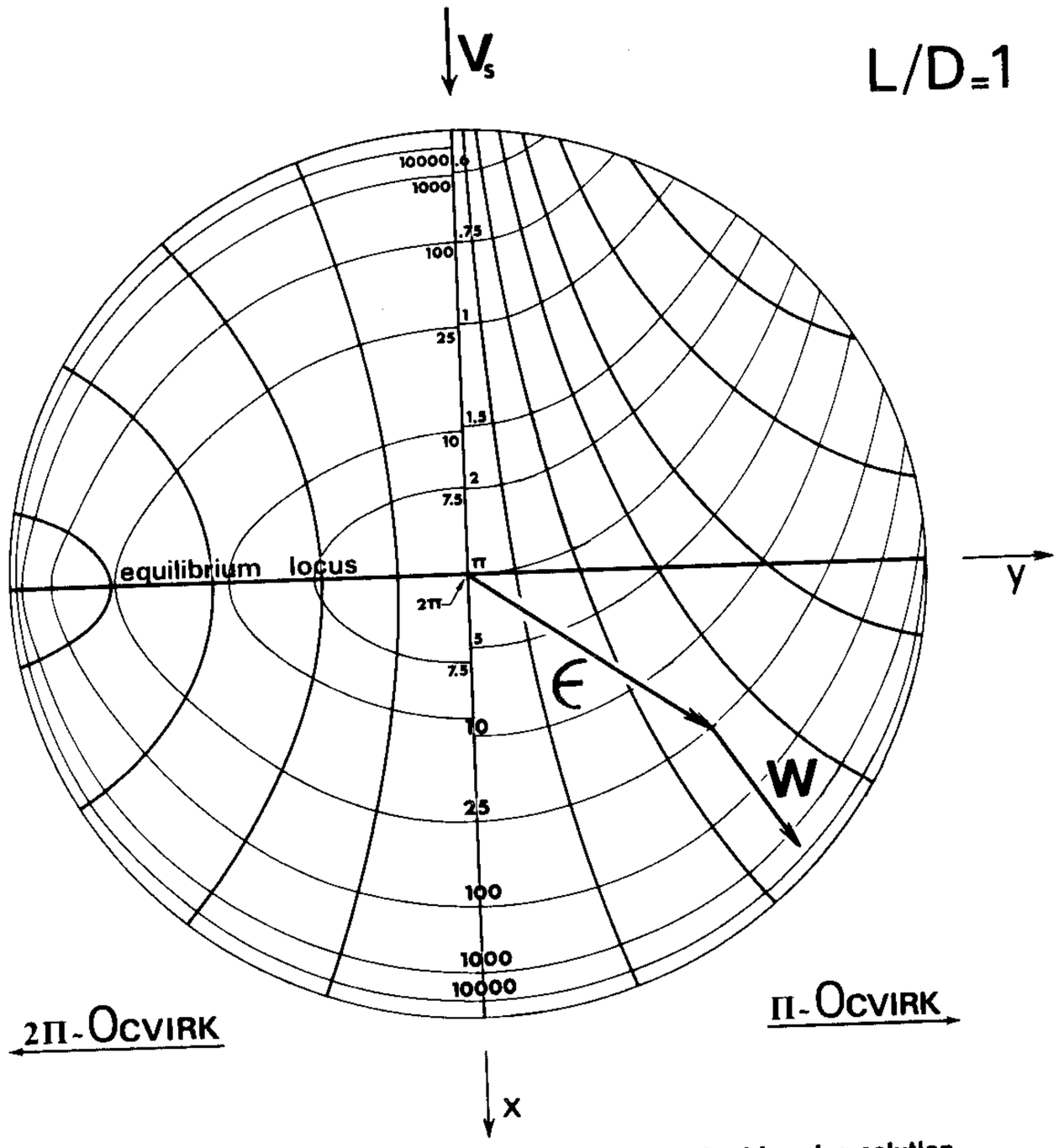

Fig. 15 Clearance circle map of impedance; short bearing solution (after Childs, Moes, and van Leeuwen)

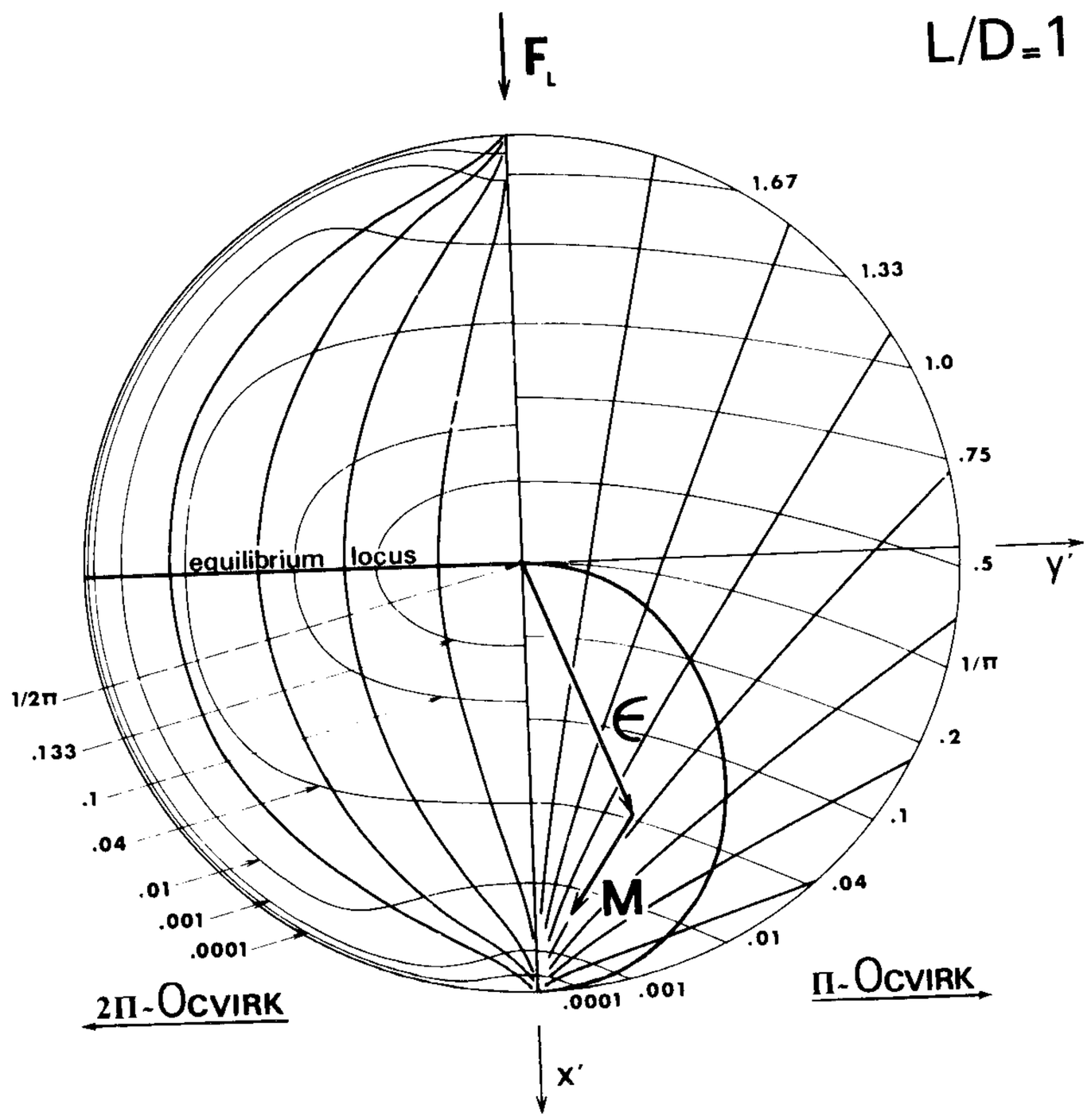

Fig. 16 Clearance circle map of mobility; short bearing solution (after Booker)

A. Impedance Method: $\mathbf{e}, \mathbf{V_S} \rightarrow \mathbf{F_L}$
Find velocity magnitude

$$|V_S| = [(V_S{}^X)^2 + (V_S{}^Y)^2]^{1/2}$$

and direction cosines

$$\begin{Bmatrix} c \\ s \end{Bmatrix} = \frac{1}{|V_S|} \begin{Bmatrix} V_S{}^X \\ V_S{}^Y \end{Bmatrix}$$

Transform eccentricity to velocity frame

$$\begin{Bmatrix} e^x \\ e^y \end{Bmatrix} = \begin{bmatrix} +c & +s \\ -s & +c \end{bmatrix} \begin{Bmatrix} e^X \\ e^Y \end{Bmatrix}$$

Find dimensionless force (impedance) in velocity (map) frame[14]

$$\begin{Bmatrix} W^x(\epsilon^x, \epsilon^y, L/D) \\ W^y(\epsilon^x, \epsilon^y, L/D) \end{Bmatrix}$$

Transform impedance to original frame

$$\begin{Bmatrix} W^X \\ W^Y \end{Bmatrix} = \begin{bmatrix} +c & -s \\ +s & +c \end{bmatrix} \begin{Bmatrix} W^x \\ W^y \end{Bmatrix}$$

Find dimensional force

$$\begin{Bmatrix} F_L{}^X \\ F_L{}^Y \end{Bmatrix} = \frac{2\mu L}{(C/R)^3} |V_S| \begin{Bmatrix} W^X \\ W^Y \end{Bmatrix}$$

B. Mobility Method: $\mathbf{e}, \mathbf{F_L} \rightarrow \mathbf{V_S}$
Find force magnitude

$$|F_L| = [(F_L{}^X)^2 + (F_L{}^Y)^2]^{1/2}$$

and direction cosines

$$\begin{Bmatrix} c' \\ s' \end{Bmatrix} = \frac{1}{|F_L|} \begin{Bmatrix} F_L{}^X \\ F_L{}^Y \end{Bmatrix}$$

Transform eccentricity to force frame

$$\begin{Bmatrix} e^{x'} \\ e^{y'} \end{Bmatrix} = \begin{bmatrix} +c' & +s' \\ -s' & +c' \end{bmatrix} \begin{Bmatrix} e^X \\ e^Y \end{Bmatrix}$$

Find dimensionless velocity (mobility) in force (map) frame[15]

$$\begin{Bmatrix} M^{x'}(\epsilon^{x'}, \epsilon^{y'}, L/D) \\ M^{y'}(\epsilon^{x'}, \epsilon^{y'}, L/D) \end{Bmatrix}$$

Transform mobility to original frame

$$\begin{Bmatrix} M^X \\ M^Y \end{Bmatrix} = \begin{bmatrix} +c' & -s' \\ +s' & +c' \end{bmatrix} \begin{Bmatrix} M^{x'} \\ M^{y'} \end{Bmatrix}$$

Find dimensional velocity

$$\begin{Bmatrix} V_S{}^X \\ V_L{}^Y \end{Bmatrix} = \frac{(C/R)^3}{2\mu L} |F_L| \begin{Bmatrix} M^X \\ M^Y \end{Bmatrix}$$

General Case: With Rotation

Extension of these impedance/mobility procedures to practical problems involving rotation of journal and/or sleeve is trivially (and surprisingly) simple:

Consider an observer fixed to the sleeve center but rotating at the average angular velocity $\bar{\omega}$ of journal and sleeve.[16,17] The actual journal center velocity $\mathbf{V}$ and the velocity $\mathbf{V_s}$ apparent to the observer are related to the journal center eccentricity $\mathbf{e}$ and the observer's angular velocity $\bar{\omega}$ by the simple kinematic expression

$$\mathbf{V} - \mathbf{V_s} = \bar{\omega} \times \mathbf{e}$$

Since the average angular velocity of journal and sleeve apparent to the observer would vanish identically, the generation of pressure and resultant force $\mathbf{F_L}$ would seem to be related solely to the apparent (squeeze) velocity $\mathbf{V_S}$ *in exactly the same way as for the non-rotating bearings considered previously.*

Thus extension of the previous numerical procedures to general problems requires only the use of the kinematic relation above in the form

$$\begin{Bmatrix} V_S{}^X \\ V_S{}^Y \end{Bmatrix} = \begin{Bmatrix} V^X \\ V^Y \end{Bmatrix} - \begin{bmatrix} 0 & -\bar{\omega} \\ +\bar{\omega} & 0 \end{bmatrix} \begin{Bmatrix} e^X \\ e^Y \end{Bmatrix}$$

before the impedance procedure, and in the form

$$\begin{Bmatrix} V^X \\ V^Y \end{Bmatrix} = \begin{Bmatrix} V_S{}^X \\ V_S{}^Y \end{Bmatrix} + \begin{bmatrix} 0 & -\bar{\omega} \\ +\bar{\omega} & 0 \end{bmatrix} \begin{Bmatrix} e^X \\ e^Y \end{Bmatrix}$$

after the mobility procedure.

A few general observations can now be made.

It is interesting to note that the *simplest* physical and analytical experiments produce mobility and impedance data respectively. Thus mobility maps (such as Fig. 16) are considerably more difficult to obtain through analytical means than are impedance maps (such as Fig. 15), and are therefore often determined from the latter as a secondary step. The preparation of either type of map is a task of considerable consequence, not likely to be undertaken for a single potential application.

In the case of the mobility map, the direction lines are in fact the path lines followed by a nonrotating journal moving in a nonrotating sleeve under the action of a nonrotating load. No analogous physical interpretation seems to arise for the impedance map. The mobility map can be used directly as the basis for a graphical determination of journal trajectories in appropriate problems. No analogous application seems obvious for the impedance map, which seems useful chiefly as a graphical summary of the numerical data it represents.

The impedance and mobility methods share limitations as well as possibilities. As noted previously, their very definitions foreclose the study of compressible films or the effect of variation of inlet pressure. Similarly, practical constraints on map development appear to limit most applications to cases with circumferential symmetry.[18] Thus little can be done with either method to study alternate inlet arrangements.

Since the mobility formulation is appropriate to cases in which instantaneous force is *known,* it has found its widest application to problems in reciprocating machinery (despite the severe limitations just cited).

Since the impedance formulation is appropriate to cases in which instantaneous force is *desired,* it seems most suited to problems in rotating machinery, particularly those involving damper bearings (thus largely evading the limitations noted). Unfortunately, however, design changes for enhanced stability of rotating machinery generally compromise bearing circumferential symmetry purposely and severely (thus imposing the limitations unavoidably).

Can the authors suggest other potential applications for the impedance (and/or mobility) method(s) which minimize the impact of inherent limitations?

Additional References

28 Blok, H., "Full Journal Bearings Under Dynamic Duty: Impulse Method of Solution and Flapping Action," JOURNAL OF LUBRICATION TECHNOLOGY, TRANS. ASME, Series F, Vol. 97, No. 2, Apr 1975, pp. 168–179.

29 Rohde, S. M., "Computational Techniques in the Analysis and Design of Fluid Film Bearings," General Motors Research Laboratories, Warren, Mich., Research Publication GMR-2279, Oct. 1976.

---

[14] Published map data is available for a variety of film models.

[15] Published map data is available for a variety of film models.

[16] The neglect of inertial effects in the derivation of the Reynolds equation assures the validity of such a rotating observer's predictions of film pressure and averaged flow.

[17] The concept of alternate observers is elaborated in the writer's paper [3], as well as in published discussion of the review by Campbell, et al [15], and in the forthcoming review by Rohde [29].

[18] Reference [26] provides a novel exception to the rule elaborated in the writer's discussion of reference [28].

P. E. Allaire[19]

The authors of this paper should be congratulated for an excellent paper transforming the mobility solution of Booker into a form more appropriate for rotor dynamics. Not only has the impedance description been developed but also it has been used for one example or another in most of the possible application areas: bearing forces, transient analysis, squeeze film dampers, dynamic coefficients, and stability. The advantages of the approach are well discussed and documented.

It appears that the major application of this type of analysis is in transient rotor dynamics. Computer time for the method is quite low, making it ideal for many repeated calculations. Thus some of the limitations encountered by Myrick and Rylander [12] in the number of nodal points at which the pressure could be evaluated can be avoided. A large portion of the paper is devoted to linearized bearing characteristics and stability but the number of times that these quantities must be evaluated for a given application is not usually large. The advantages of the more general finite differences or finite elements are likely to justify the longer running time.

One of the disavantages of the approach described here for plain journal bearings is that the combination of short and long bearing solutions has been shown to be accurate for a number of cases but there is no method presented for estimating the error. If a set of journal positions and velocities were encountered where substantial errors occured, only comparison with a different numerical or analytical finite length solution would show the error. No method analogous to adding more nodes or another term of an infinite series and observing the change in force (for example) appears to be available.

Suggested extensions of the mobility-impedance analysis procedure include lobed bearings for which all lobes are at high eccentricity ratios. Perhaps it should be pointed out that no short bearing analysis exists for partial arc or lobed bearings due to the boundary conditions at the end of the lobes. Thus the present method of a weighted combination of short and long bearing solutions is not possible.

An alternative approach to the methods discussed in this work is that of Hays [30, 31][20] where a variational principle equivalent to Reynolds' equation is minimized with an infinite trigonometric series for the pressure. This method can be generalized to the full dynamic conditions for either a squeeze film damper or plain journal bearing. Because of the relatively simple trigonometric nature of the integrals for the force on the journal, an algebraic series solution to the finite length journal bearing results. Running time is comparable to that for the short bearing. The method is also applicable to partial arc, multilobe and other types.

Additional References

30 Hays, D. F., "Squeeze Films: A Finite Journal Bearing with A Fluctuating Load," *Journal of Basic Engineering*, TRANS. ASME, Series D, Vol. 83, Dec., 1961, pp. 579–588.

31 Hays, D. F., "A Variational Approach to Lubrication Problems and the Solution of the Finite Journal Bearing," *Journal of Basic Engineering*, TRANS ASME, Series D, Vol. 81, Mar., 1959, pp. 13–23.

Author's Closure

Professor Booker's additional clarifying comments on the relationships of the mobility and impedance vectors and the basic limitations of the methods are appreciated. In response to Professor Booker's question concerning the inherent limitations of the methods, the authors suggest the following additional applications for the methods:

(*a*) **Squeeze-Film Damper Coefficients.** In addition to the damper coefficient formulas of Tonneson [9] given in equation (55), for circular orbits the stiffness and damping coefficients of equations (47) and (50) can be used to define "equivalent" linear stiffness and damper coefficients for a damper. Specifically, appropriate stiffness and damping coefficients are

$$K_d = a_{\epsilon\epsilon} = 2\mu L \left(\frac{R}{C}\right)^3 \epsilon_0 \dot{\phi}_0 \left\{\frac{W_\epsilon(\epsilon_0, \alpha_0)}{\epsilon_0} + \frac{\partial W_\epsilon(\epsilon_0, \alpha_0)}{0\epsilon}\right\}$$

$$C_d = b_{\beta\beta} = 2\mu L \left(\frac{R}{C}\right)^3 |W_\beta(\epsilon_0, \alpha_0)|$$

where $\alpha_0 = \pi/2$ for clockwise rotation, and $\alpha_0 = -\pi/2$ for counterclockwise rotation. This formula for K_d differs from that employed by Cunningham, et al. [32], who use the following "average" definition, $K_d \simeq -F_\epsilon/C\epsilon_0 = 2\mu L(R/C)^3 \dot{\phi}_0 W_\epsilon(\epsilon_0, \alpha_0)$

(*b*) **Pivoted Pad Bearings.** Impedance descriptions have been developed for the rectilinear Michell pad bearing, and will be included in a forthcoming publication. At present, impedance descriptions can be calculated for radial pivoted pads [26], which means that transient simulations may be carried out for rotors supported in pivoted-pad bearings. However, the prospects for finding accurate analytic approximations for a radial pivoted pad impedance are not encouraging, which implies that the derivation of analytic stiffness and damping coefficients for this type of bearing from impedances is also unlikely.

Professor Allaire's inquiries concerning the potential accuracy of the impedances provided for finite-length bearings can best be answered by a careful review of the methods employed for their derivation. The impedances provided are based on previously calculated mobilities, which were obtained by numerical solution of the Reynolds equation for finite-length bearings over a range of L/D ratios. The observation was made that a very accurate analytic approximation to these mobilities could be obtained from a weighted sum of short and long bearing solutions. At the equilibrium locus, the analytical impedance solutions are less than .1 percent in error when compared to impedances calculated from either finite difference or finite-element methods. The authors regret any implication that these same functions could be employed to approximate numerically calculated impedances for other types of bearings.

With regard to the method of Hays [30], [31], this method has been applied to finite length bearings for 2π and π regions of positive pressure. The application of this method for the more accurate ($p = \partial p/\partial\theta = 0$) cavitating boundary conditions appears to the authors to be a very difficult undertaking. A solution based on these boundary conditions would be required to obtain a bearing model comparable in accuracy to the finite-length cavitating impedance of equations (29)–(32).

The authors fail to see the advantages suggested by Professor Allaire for calculating stiffness and damping coefficients for a plain journal bearing by numerical methods, when compared to simply evaluating the formulas of equations (53) and Appendix B. In our opinion, the formulas can be evaluated much more quickly, and provide comparable accuracy.

Additional References

[32] Cunningham, R. E., Fleming, D. P., and Gunter E. J., "Design of a Squeeze-Flim Damper for a Multimass Flexible Rotor," *Journal of Engineering for Industry*, TRANS. ASME, Nov. 1975, pp. 1383–1389.

---

[19] Assistant Professor Mechanical Engineering Department, University of Virginia, Charlottesville, Va.

[20] Numbers 30–31 in brackets designate Additional References at end of discussion